Simultaneous identification of structural parameters and dynamic loads in time-domain using partial measurements and state-space approach

Zakaria Bitro[a], Anas Batou[a,b,*], Huajiang Ouyang[a]

[a] *Department of Mechanical, Materials and Aerospace Engineering, School of Engineering, University of Liverpool, Liverpool L69 7ZF, United Kingdom*
[b] *MSME, Univ Gustave Eiffel, CNRS UMR 8208, Univ Paris Est Creteil, F-77474 Marne-la-Vallée, France*

Abstract

Structural identification is an essential process in structural health monitoring, condition assessment and structural safety evaluation. This inverse problem becomes more challenging when information on the dynamic loads is missing or not fully known. Hence, it is important to establish methods to identify structural parameters and dynamic loads simultaneously from the measured structural responses which are easy to obtain compared to dynamic loads. This paper proposes a novel method to identify simultaneously structural parameters and dynamic loads from structural responses measured on a limited set of degrees-of-freedom. Firstly, an objective function is defined as the difference between the measured structural responses and the theoretically computed responses, and then the derivative of the residual function with respect to structural parameters is calculated numerically using the forward-difference method. The derivative of the residual function with respect to the external dynamic loads is computed using the state-space formulation and the system matrix composed of Markov parameters to facilitate the derivative-based identification. Secondly, the nonlinear optimization problem is solved using the Levenberg-Marquardt algorithm. Several numerical examples are analysed to demonstrate the effectiveness and robustness of the method. Finally, the effect of initial estimates of the parameters and dynamic loads and the effect of measurement noise, as well as the effects of number of measurements are investigated. The proposed method is also shown to achieve a satisfactory solution even when the initial estimates of parameters and dynamic loads are far from their true values.

Keywords: structural dynamics, parameter identification, dynamic load identification, Levenberg-Marquardt algorithm

1. Introduction

Civil engineering structures withstand various types of dynamic loads during their service life. As a result, structural identification and dynamic load quantification become crucial elements in the critical evaluation of structural health and safety. Conventionally, vibration-based structural identification is performed in either frequency domain or time domain [1, 3, 9]. Frequency domain approaches rely on changes in natural frequencies and mode shapes as well as their derivatives to update the numerical models [24] or to identify damage using these global structural quantities [28]. Time-domain identification methods on the other hand are more versatile in enabling the identification of transient loads. Methods based on least-squares have been studied for a relatively long time [4, 17, 34, 35, 15, 13], in which satisfactory identification results were obtained. However, simultaneous identification methods based on iterative least-squares will usually have special requirements such as measurements from all degrees-of-freedom. This will greatly restrict their application since it is not feasible to have sensors measuring all the degrees-of-freedom of a structure. To circumvent this limitation, popular approaches

*Corresponding author
Email address: batoua@liverpool.ac.uk (Anas Batou)

based on extended-Kalman filter were proposed [8, 19, 20, 26, 6, 16, 31]. The extended-Kalman filter has proved to be a powerful tool for the identification of structural parameters and dynamic loads and promising results were obtained, however, the procedure of the extended-Kalman filter requires the linearization of the nonlinear extended state vector, this may cause stability issues in the identification of structural parameters. Furthermore, low-frequency drift in the identified dynamic loads and updated states when the extended-Kalman filter is used was also reported [20]. Another famous approach is sensitivity-based structural identification [24, 32, 37, 21, 5]. This method which is effective and convenient to implement, enables satisfactory results to be obtained for simultaneous identification of dynamic loads and structural parameters. Nevertheless, a downside of the sensitivity-based structural identification approach is that a good initial estimate must be provided for the structural parameters and dynamic loads. This is restrictive because in most practical cases there might be a lack of information about the true values of the structural parameters and dynamic loads and a large range of variation must be allowed in the initial estimates before starting the identification process. Recently, approaches based on deep neural networks became more popular for the identification of parametric models and dynamic loads [18, 39, 36]. The deep learning based methods are powerful and can provide accurate results, but they require large amount of data to train the network and may result in overfitting of the trained data. Furthermore, the deep learning models may not be capable of simultaneous identification of dynamic loads and structural parameters in case of complex transient loads that require a large number of input parameters to be represented accurately. Other general approaches were also reported in the literature in order to identify structural parameters and dynamic loads, since there is a vast amount of literature on the identification of structural parameters and dynamic loads, this paper will only cite some prominent papers that are concerned mainly with the simultaneous identification of dynamic loads and structural parameters.

Feng et al.[12] used state-space modelling and Gauss-Newton method to identify bridge structural parameters and vehicle axle loads, in their study, only partial acceleration measurements were used in the identification process. Bayesian inference regularization was used to solve the ill-posed least-squares problem when identifying the axle loads. Sun et al.[30] proposed a two-step simultaneous identification approach in time domain to identify structural parameters and dynamic loads. Statistical Bayesian regularization was used to solve the ill-posed least-squares problem associated with dynamic loads identification. Zhu et al.[40], proposed a sensitivity based structural damage and dynamic loads identification using the transmissibility concept. The transformation matrix was established using the state-space matrix composed of Markov parameters, and the relationship between two sets of acceleration response measurements was established without the need for dynamic load information. Furthermore, the sensitivity of dynamic response with respect to change in stiffness was derived analytically to identify damage in the structure. Sun and Betti [29] presented a hybrid heuristic optimization algorithm that combined the artificial bee colony and local search operator to identify structural parameters and the dynamic loads. More recently, Wang et al.[33] used a perturbation method to identify structural parameters and dynamic loads using partial measurements. The impulse response matrix was expanded using perturbation theory and the dynamic load was decomposed via orthogonal expansion. Finally, the orthogonal coefficients and changes in the parameters were identified by least-squares and Tikhonov regularization methods. Jayalakshmi and Rao [14] used the dynamic adaptive firefly optimization algorithm and the explicit form of the Newmark-β method for simultaneous identification of dynamic loads and structural parameters. A modified Tikhonov regularization method was used to reduce the ill-posedness associated with dynamic load identification. Zhang et al.[38] proposed novel method to identify structural damage and dynamic loads simultaneously, the virtual distortion method was adopted to reduce the computational cost and to compute the impulse response of the damaged structure, the approach was validated numerically as well as experimentally. Feng et al.[11] proposed a novel method for simultaneous identification of stiffness parameters and dynamic loads. A non-contact vison based displacement sensor was used in their study, this type of sensors is economical and provide accurate estimation of the displacement on specific points defined by the researcher. Finally, the structural stiffness parameters and dynamic loads are identified using optimisation techniques. Chen et al.[5] used Bayesian based approach for simultaneous identification of structural damage and input dynamic load. The dynamic

load was expended via orthogonal polynomials and and the posterior probability density function of the orthogonal coefficients and damaged parameters were deduced in time domain using Bayesian theory combined with Laplace approximation. Pan et al.[25] used a novel approach for simultaneous identification of dynamic loads and structural damage, The optimisation problem was divided to several sub-tasks to reduce the computational complexity and storage. Each sub-task is then solved more easily than the original problem. Finally, the damage coefficients and impact dynamic loads are obtained via sparse regularization. To reduce the false positives in damage indices, zhang et al.[37] proposed a probabilistic method for simultaneous identification of dynamic loads and structural damage. Firstly, the deterministic approach is firstly established to identify the structural damage parameters and the orthogonal coefficients of the dynamic load. Secondly, the probability theory is used to obtain the statistical information of the damage parameters and dynamic load. Pourzeynali et al.[27] combined the explicit form of the Newmark-β and the sensitivity-based structural damage identification with Tikhonov regularization to identify simultaneously the structural damage and axle loads, the applicability of the proposed method was also verified experimentally. To sum up, most of the existing simultaneous identification methods are computationally challenging or complicated to be implemented or the method may need special requirements to start the identification process.

The present paper proposes a new method to simultaneously identify structural parameters and dynamic loads using partial response measurements of acceleration and displacement. Firstly, the objective function defined as the least-squares difference between the measured responses and the theoretically computed responses is derived. Secondly, the non-linear optimization problem is solved with the Levenberg-Marquardt algorithm in the state-space. The derivative of the residual function with respect to structural parameters is derived numerically using a forward-difference scheme, and the derivative of the residual with respect to the external dynamic loads is established using the system matrix derived from state-space and composed of Markov parameters, which represents the impulse response of the system. This paper is organised as follows: Section 2 introduces the state-space formulation as well as the simultaneous identification of structural parameters and dynamic loads as an optimization problem. Section 3 presents numerical studies to demonstrate the effectiveness and robustness of the proposed method. Section 4 provides an experimental validation of the proposed approach. Section 5 provide concluding remarks to summarize the main outcomes of this study.

2. Simultaneous identification of structural parameters and dynamic loads

2.1. State-Space Formulation

We consider the n-Dof system for which the computational model (obtained by the Finite Element method or using discrete masses) is represented by the following matrix differential equation

$$[M]\,\ddot{\mathbf{x}}(t) + [C]\,\dot{\mathbf{x}}(t) + [K]\,\mathbf{x}(t) = [L]\,\mathbf{f}(t), \tag{1}$$

in which the $(n \times n)$ matrices $[M], [C], [K]$ respectively represents the mass, damping and stiffness matrices of the structure, the n-dimension vectors $\ddot{\mathbf{x}}(t)$,$\dot{\mathbf{x}}(t)$,$\mathbf{x}(t)$ are respectively the acceleration, velocity and displacement of the structure. $\mathbf{f}(t)$ is the n_r dimension vector of external dynamic loads where n_r is the number of external dynamic loads acting on the structure. $[L]$ is the $(n \times n_r)$ input influence matrix which associates the n_r external dynamic loads to the corresponding DoF on the structure. Equation (1) can be represented in state-space form as follows

$$\dot{\mathbf{z}}(t) = [A]\,\mathbf{z}(t) + [B]\,\mathbf{f}(t), \tag{2}$$

where the state vector $\mathbf{z}$(t) is defined as

$$[\mathbf{x}(t), \dot{\mathbf{x}}(t)]^{\mathrm{T}}, \tag{3}$$

in which the matrices $[A]$ and $[B]$ are defined as:

$$[A] = \begin{bmatrix} [0] & [I] \\ [M^{-1}][K] & [M^{-1}][C] \end{bmatrix}, \qquad [B] = \begin{bmatrix} [0] \\ [M^{-1}][L] \end{bmatrix}, \tag{4}$$

where [I] is the identity matrix. The output vector $\mathbf{y}(t)$ of the n_s measured DoFs used in the identification is defined as

$$\mathbf{y}(t) = [R_a]\ddot{\mathbf{x}}(t) + [R_v]\dot{\mathbf{x}}(t) + [R_d]\mathbf{x}(t), \tag{5}$$

where $[R_a], [R_v], [R_d]$ are the output influence matrices of the acceleration, velocity and displacement respectively. They all have a dimension of $(n_s \times n)$. In this paper, a data fusion method of acceleration and displacement measurements is used in the identification procedure to circumvent the effect of low-frequency drift on the identified dynamic loads, and therefore the term $[R_v]\,\dot{\mathbf{x}}(t)$ is not considered. Equation(5) can be rewritten as the following

$$\mathbf{y}(t) = [Q]\mathbf{z}(t) + [D]\mathbf{f}(t), \tag{6}$$

where $[Q]$ and $[D]$ are defined as

$$[Q] = \left[[R_d] - [R_a][M^{-1}][C], -[R_a][M^{-1}][K]\right],\ [D] = \left[[R_a][M^{-1}][L]\right]. \tag{7}$$

Equations (2) and (6) represents a continuous-time state-space model and can be discretised in the time domain using the following scheme

$$\mathbf{z}_{k+1}(t) = [A_d]\mathbf{z}_k(t) + [B_d]\mathbf{f}_k, \tag{8}$$

in which Δt is the time step and where $[A_d], [B_d]$ can be computed using the exponential matrix algorithm as follows

$$[A_d] = \mathrm{e}^{[A]\Delta t}, \qquad [B_d] = [A]([A_d] - [I])^{-1}[B]. \tag{9}$$

Similarly, the measurement equation is also discretised as given in the following expression

$$\mathbf{y}_k = [Q]\mathbf{z}_k + [D]\mathbf{f}_k. \tag{10}$$

Upon substituting Eq.(8) into Eq.(10), taking the unit impulse of the load at $k = 0$ and taking the load to be zero at $k \geq 1$, the following equation is obtained

$$\hat{\mathbf{y}} = [H]\hat{\mathbf{f}}, \tag{11}$$

in which $\hat{\mathbf{y}}$ is the concatenation of vectors $\mathbf{y}_1, \ldots, \mathbf{y}_{nt}$ and where $\hat{\mathbf{f}}$ is the input vector constructed as the concatenation of the dynamic loads vector $\mathbf{f}_1, \ldots, \mathbf{f}_{nt}$ with n_t denoting the number of the total time increments. In Eq.(11), $[H]$ is the $(n_s\, n_t \times n_r\, n_t)$ system matrix, which is composed of the system Markov parameters. These parameters represent the response of the discrete linear dynamical system to a unit impulse and therefore this matrix is unique for each given system. The system matrix can be computed based on the following expressions

$$[H_o] = [D], \qquad [H_i] = \sum_{i=1}^{n_t - 1} [Q][A_d^{i-1}][B_d]. \tag{12}$$

The block representation of Eq.(11) reads

$$\begin{bmatrix} \mathbf{y}_1 \\ \mathbf{y}_2 \\ \mathbf{y}_3 \\ \vdots \\ \mathbf{y}_{nt} \end{bmatrix} = \begin{bmatrix} [H_o][L] & [0] & \ldots & \ldots & [0] \\ [H_1][L] & [H_o][L] & \ldots & \ldots & [0] \\ [H_2][L] & [H_1][L] & [H_o][L] & \ldots & \ldots \\ \vdots & \vdots & \vdots & \vdots & \vdots \\ [H_{nt-1}][L] & [H_{nt-2}][L] & \ldots & \ldots & [H_o][L] \end{bmatrix} \begin{bmatrix} \mathbf{f}_1 \\ \mathbf{f}_2 \\ \mathbf{f}_3 \\ \vdots \\ \mathbf{f}_{nt} \end{bmatrix}. \tag{13}$$

Based on Eq.(13), if the structural parameters are all known, and the dynamic response of the structure from specified sets of sensors are provided, then the unknown dynamic loads time history $\hat{\mathbf{f}}$ can be determined by solving Eq.(13) using the pseudo-inverse of matrix $[H]$. However, this is an ill-posed inverse problem, particularly when the measured responses are contaminated with noise. The ordinary least-squares solution may yield unbounded or poor results, necessitating the use of regularization to stabilize the solution process.

2.2. Simultaneous Identification algorithm

The proposed approach can generally be used to identify some of the structural parameters and dynamic loads. In other words, some parameters are assumed to be known and only partial parameters will be simultaneously identified with dynamic loads. Identifiable parameters include all stiffness- and damping- related parameters, as will be shown in section 4. However, the mass-related parameters can not be identified by the proposed approach.

Let $\boldsymbol{\theta}$ be the vector of the n_p system parameters to be estimated. Then Eq.(11) can be rewritten as

$$\hat{\mathbf{y}}(\boldsymbol{\theta}, \hat{\mathbf{f}}) = [H(\boldsymbol{\theta})]\hat{\mathbf{f}}. \tag{14}$$

The residual vector is defined as

$$\mathbf{r}(\boldsymbol{\theta}, \hat{\mathbf{f}}) = \hat{\mathbf{y}}^{\text{mes}} - \hat{\mathbf{y}}(\boldsymbol{\theta}, \hat{\mathbf{f}}), \tag{15}$$

where $\mathbf{y}^{\text{mes}}$ is the vector of the concatenated measured responses. The objective is to minimize the residual in Eq.(14) by finding the optimal values of the system parameters and dynamic loads that will bring the estimated responses as close as possible to the measured structural responses. Vectors $\boldsymbol{\theta}$ and $\hat{\mathbf{f}}$ are the estimated parameters and dynamic loads respectively. The objective function $\eta(\boldsymbol{\theta}, \hat{\mathbf{f}})$ to be minimised is expressed as the least squares of the residual vector as shown in the following expression

$$\eta(\boldsymbol{\theta}, \hat{\mathbf{f}}) = \mathbf{r}(\boldsymbol{\theta}, \hat{\mathbf{f}})^{\mathrm{T}}\mathbf{r}(\boldsymbol{\theta}, \hat{\mathbf{f}}). \tag{16}$$

The optimal values $\boldsymbol{\theta}^{\,\text{opt}}$ and $\mathbf{f}^{\,\text{opt}}$ for the system parameters and the dynamic loads are then the solutions of the following optimization problem

$$(\boldsymbol{\theta}^{\,\text{opt}}, \mathbf{f}^{\,\text{opt}}) = \underset{\theta \in \mathcal{C}_\theta,\ \hat{\mathbf{f}} \in \mathcal{C}_f}{\operatorname{argmin}} \ \eta(\boldsymbol{\theta}, \hat{\mathbf{f}})\,, \tag{17}$$

where $\mathcal{C}_\theta$ and $\mathcal{C}_f$ are the admissible search spaces for the system parameters and the dynamic loads respectively. Eq.(17) corresponds to a nonlinear optimization problem, and the Levenberg-Marquardet algorithm is proposed to solve it until a sufficiently small error is reached. The Levenberg-Marquardt method is an interpolation between the gradient descent method and the Gauss-Newton method. It is proposed to circumvent the problem of rank deficiency and singularity by introducing the damped version of the Gauss-Newton method. The algorithm is described by the following iteration scheme

$$\boldsymbol{\theta}_{i+1} = \boldsymbol{\theta}_i + ([J_\theta]^{\mathrm{T}}[J_\theta] + \alpha\,\mathrm{diag}([J_\theta]^{\mathrm{T}}[J_\theta]))^{-1}[J_\theta]^{\mathrm{T}}\boldsymbol{r}(\boldsymbol{\theta}_i, \hat{\mathbf{f}}_i), \tag{18}$$

$$\hat{\mathbf{f}}_{i+1} = \hat{\mathbf{f}}_i + ([J_f]^{\mathrm{T}}[J_f] + \gamma\,\mathrm{diag}([J_f]^{\mathrm{T}}[J_f]))^{-1}[J_f]^{\mathrm{T}}\boldsymbol{r}(\boldsymbol{\theta}_i, \hat{\mathbf{f}}_i), \tag{19}$$

where $[J_\theta]$ and $[J_f]$ are the Jacobian matrices of the residual vector with respect to the structural parameters and dynamic loads respectively. α and γ are the damping parameters, precise determination of these parameters is an essential step in the proposed method, more details can be found in section 2.4. Equations (18) and (19) represent the iteration process of the identification algorithm. It is noted that this is not a 2-step method, and the dynamic loads and structural parameters are both evaluated based on the previous iteration. Therefore, to start the identification process, an initial estimate of both the structural parameters and dynamic loads is required. It will be shown that the method is robust to these initial estimates, indicating the versatility of the proposed method and its applicability for practical application. The most challenging part of the algorithm is the accurate calculation of the Jacobian matrix as it will determine the searching direction of the optimisation process.

2.3. Calculation of the derivatives

Using Eq.(15), the derivative of the residual vector with respect to the ith structural parameter is given as:

$$\frac{\partial \boldsymbol{r}}{\partial \theta_i} = -\frac{\partial \hat{\mathbf{y}}(\boldsymbol{\theta}, \hat{\mathbf{f}})}{\partial \theta_i}. \tag{20}$$

It is possible now to evaluate Eq.(20) based on two approaches. The first approach is to directly differentiate Eq.(1) with respect to the structural parameter that needs to be identified, leading to following expression [21]

$$[M]\frac{\partial \ddot{\boldsymbol{x}}}{\partial \theta_i} + [C(\boldsymbol{\theta})]\frac{\partial \dot{\boldsymbol{x}}}{\partial \theta_i} + [K(\boldsymbol{\theta})]\frac{\partial \boldsymbol{x}}{\partial \theta_i} = -\frac{\partial [K(\boldsymbol{\theta})]}{\partial \theta_i}\boldsymbol{x}_e - \frac{\partial [C(\boldsymbol{\theta})]}{\partial \theta_i}\dot{\boldsymbol{x}}_e, \tag{21}$$

where matrices $[K(\boldsymbol{\theta})]$ and $[C(\boldsymbol{\theta})]$ are the estimated stiffness and damping matrices at each iteration. Vectors $[\dot{\boldsymbol{x}}_e,\boldsymbol{x}_e]$ are respectively the theoretically computed velocity and displacement vectors from the FE model. The right-hand side of Eq.(21) may be considered an equivalent forcing function, and the dynamic response sensitivity may be computed numerically using the Newmark-β method. Alternatively, Eq.(20) can be evaluated using forward difference method as

$$\frac{\partial \boldsymbol{r}}{\partial \theta_i} \simeq \frac{\boldsymbol{r}(\theta_i + \delta\theta_i, \hat{\mathbf{f}}) - \boldsymbol{r}(\theta_i, \hat{\mathbf{f}})}{\delta\theta_i}. \tag{22}$$

Which is more desirable when using a commercial software package or when the structure is complicated and a direct differentiation may be expensive to compute at each iteration of the solution process. Therefore, in this paper the forward difference scheme is used as the main derivative computation method. Particularly, the residual vector is firstly computed without perturbing the ith structural parameter, and then the ith structural parameter is allowed to have a small perturbation from its original value. Then the residual is calculated after the perturbation and Eq.(22) is used to compute the derivative of the residual with respect to the ith structural parameter. The partial derivative for each parameter can then be assembled into a matrix form depending on n_p parameters to be identified as follows:

$$\frac{\partial \boldsymbol{r}}{\partial \boldsymbol{\theta}} = \left[\frac{\partial \boldsymbol{r}(\theta_1)}{\partial \theta_1} \quad \frac{\partial \boldsymbol{r}(\theta_2)}{\partial \theta_2} \quad \cdots \quad \frac{\partial \boldsymbol{r}(\theta_{n_p})}{\partial \theta_{n_p}}\right]. \tag{23}$$

Equation (23) can then be directly used in Eq.(18) to estimate the new set of structural parameters. The derivative of the residual function with respect to the estimated dynamic loads must also be determined to identify new and improved estimate of dynamic loads. From Eq.(14), it can be seen that the relationship between the estimated response and the estimated dynamic loads can be established through a state-space model, where the Markov parameter matrix is composed of the estimated set of parameters. It is now possible to formulate the Jacobian matrix $[J_f]$ of the residual. Using Eq.(14) the partial derivative of the residual with respect to the dynamic loads reads

$$\frac{\partial \boldsymbol{r}(\boldsymbol{\theta}, \hat{\mathbf{f}})}{\partial \hat{\mathbf{f}}} = -\frac{\partial \widetilde{\mathbf{y}}(\boldsymbol{\theta}, \hat{\mathbf{f}})}{\partial \hat{\mathbf{f}}}, \tag{24}$$

which is directly obtained as

$$\frac{\partial \mathbf{r}(\boldsymbol{\theta}, \hat{\mathbf{f}})}{\partial \hat{\mathbf{f}}} = -[H(\boldsymbol{\theta})]. \tag{25}$$

2.4. Determination of damping parameters

The Levenberg-Marquardt algorithm provides stable and robust performance and improved convergence by introducing a damping parameter, which is modified in each iteration [23, 10, 22, 7]. It is recommended to use large values for the damping parameter at the beginning of the solution process to allow the method to achieve the desired gradient descent characteristics and achieve a rapid reduction in the residual [23]. As the solution improves, the damping parameter is reduced gradually to adopt the characteristics of Gauss-Newton method which achieves fast and robust convergence when the values of the optimization variables are in the vicinity of the true values [23]. In this paper, two damping parameters must be determined as shown in Eq.(18) and (19), a careful selection of these parameters is of a critical importance for the identification accuracy and convergence. Several approaches have been reported in the literature for suitable choice for the damping parameter. Levenberg and Marquardt [23] proposed the adaptive tracking technique to reduce or increase the damping parameter such that faster

and stable convergence is achieved. More recently, Fan and Pan [10] proposed a more general approach to choose an appropriate damping parameter, the general form is given as follows

$$\beta_i = \lambda(||\mathbf{r}_i||) + (1-\lambda)(||[J_i]\mathbf{r}_i||), \tag{26}$$

where $\lambda \in [0,1]$, and the Jacobian matrix and the residual vector are updated at each iteration. It is expected that as the results of the identified structural parameters and dynamic load converge, the parameters α and γ provided in Eq. (18) and (19) will be smaller but Eq.(26) will guarantee bounded values of these two damping parameters and prevent them from being too small and cause stability issue during the identification process. This is very important particularly when the measured responses are contaminated with random noise, therefore, Eq.(26) is chosen in this paper to determine the two damping parameters. A detailed study on suitable selection of the damping parameter is provided by Ma and Jiang [22].

2.5. Data fusion of acceleration and displacement

If only the acceleration measurements are used in the identification process, a low-frequency drift may be observed on the identified dynamic loads which then deviate from the optimal solution, especially when the measured responses are contaminated with random noise. Acceleration measurements contain high-frequency characteristics, whereas displacement measurements are more robust to noise. Using a combination of the acceleration and the displacement measurements (not necessarily on the same dof) in the identification, the low-frequency drift that can occur in the identified dynamic loads is reduced or eliminated. It should be noted that using signal post-processing and data filtering may also lead to an improved results. The overall procedure of the proposed method is summarised as follows:

1. Conduct the dynamic test on the structure and collect measured responses and estimate the initial values of the parameters and dynamic loads as $\boldsymbol{\theta}_o$ and $\hat{\mathbf{f}}_o$.
2. Build the system matrix $[H]$ in Eq.(11).
3. Calculate the derivative of residual with respect to structural parameters and dynamic loads from Eq.(22) and Eq.(25) and calculate the two damping parameters from Eq.(26).
4. Update the dynamic load and the structural parameters using Eq.(18) and Eq.(19), and update the structural matrices.
5. Update the estimated responses and calculate new residual vector and update the Jacobain matrices and the two damping parameters.
6. Repeat steps (2)-(5) until convergence criterion is met.

The stopping criterion for the algorithm is set as follows

$$\frac{||\boldsymbol{\theta}_{i+1} - \boldsymbol{\theta}_i||}{||\boldsymbol{\theta}_{i+1}||} + \frac{||\mathbf{f} - \hat{\mathbf{f}}_i||}{||\mathbf{f}||} \leq \epsilon, \tag{27}$$

where ϵ is a small constant number that needs to be defined by the user and is problem dependent.

A flow chart of the proposed method is provided in Figure 1. before analysing the performance of the proposed approach, the following remarks are intended to clarify important points in the proposed study.

It should be noted that there exist no relationship between the number of measurements points and the number of parameters to be identified. Generally, more measurements will yield better identification results. However, a necessary requirement is that the number of measurements must be greater than the number of dynamic loads to be identified to ensure the condition of overdetermination when identifying the dynamic loads. Furthermore, the proposed approach is only applicable to parametric system identification problems, it can not be used for the identification of non-parametric models.

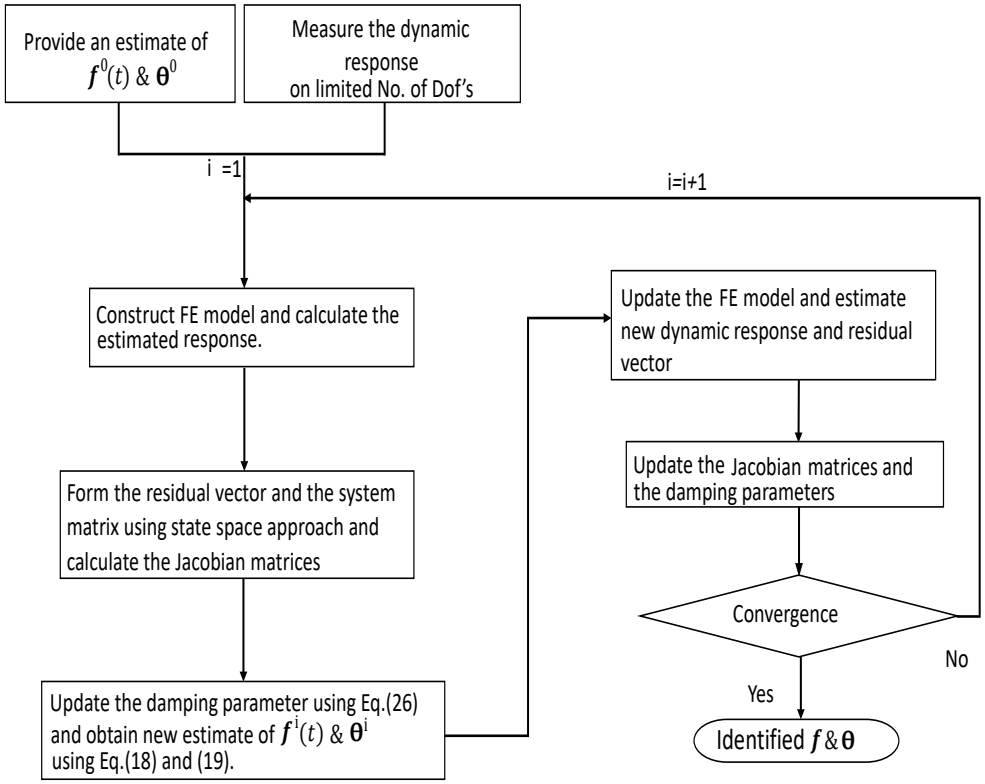

Figure 1: Flow chart for the proposed method

Figure 2: A cantilever beam structural model

3. Numerical validation

To demonstrate and validate the performance of the proposed method, several numerical examples are analysed in detail to simultaneously identify structural parameters and dynamic loads using partially measured structural responses. The structural mass matrix is assumed given in these examples and will not be identified. In engineering applications, it is not difficult, in general, to obtain a good approximation of the mass properties of a structure. For all the examples, the measured experimental responses are generated numerically. The impact of the experimental noise is analysed.

3.1. A Cantilever beam under tip load

This section is concerned with the analysis of a cantilever beam depicted in Figure 2. The beam is numerically modeled using 12 Euler beam elements, with each element having a length of 1 m. There are a total of 13 nodes, resulting in 36 dof (axial, lateral and rotation at each node) for the beam model. The left-end of the beam is fixed and a dynamic load $\mathbf{f}(t)$ is applied on the right-end. The Young's modulus is $E = 210$ GPa , the cross-sectional area is $A = 0.1 \times 0.1\,\mathrm{m}^2$, the mass density is $\rho = 7800\,\frac{\mathrm{kg}}{\mathrm{m}^3}$. A Rayleigh damping model is used in this example, the damping matrix can then be expressed as $[C] = a[M] + b[K]$ with $a = 0.4035$ and $b = 0.0032$, providing approximately 5% damping ratio for the first two elastic modes. A harmonic dynamic load is used in this example with multiple harmonic components. This load is defined as follows

$$\begin{aligned}\mathbf{f}(t) = 600\sin(12t) - 100\sin(8.5t) + 120\sin(13.4t)\\ -400\cos(15.5t) + 200\cos(11.345t).\end{aligned} \tag{28}$$

The time history of the dynamic load is shown in Figure 3.

The Newmark-β method is used for the forward analysis (to get the numerical measured responses), with a time step of 0.002 second, the response is calculated for a duration of 2 seconds. Four measurements are used in total for the identification process, two acceleration measurements and two displacement measurements, to eliminate the low-frequency drift of the identified dynamic load. The first acceleration measurement corresponds to the vertical linear acceleration measured at a distance 7 m from the left-end and the second acceleration measurement corresponds to the vertical linear acceleration measured at a distance 12 m from the left-end, only linear acceleration is used because they can be obtained more easily than angular acceleration. The two displacements are linear vertical displacements measured at a distance 4 m and 8 m from the left-end respectively.

Table 1: True values and initial estimates of each bending stiffness

Parameter	True value(Nm^2)	Initial estimate(Nm^2)
EI_1	2.8×10^6	1.8×10^6
EI_2	1.75×10^6	1.225×10^6
EI_3	5.25×10^6	3.675×10^6

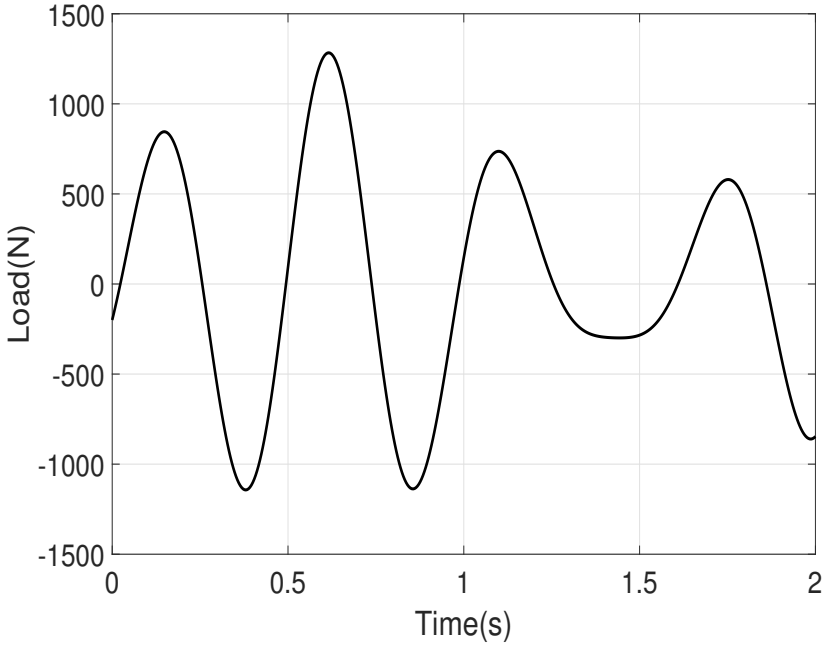

Figure 3: Dynamic load time history

The chosen structural parameters that will be identified in this example are the bending stiffnesses. The damping parameters are all assumed to be known and will not be identified in this application. The beam is divided into three parts each having a different bending stiffness. Table 1 lists their values, as well as their initial estimates which were used in the identification process. The time history of the dynamic load will also be identified simultaneously with the structural parameters. The dynamic load is assigned an arbitrary constant value of 100 N which is completely different from the dynamic load given in Eq.(28). To quantify the error in the structural parameters and dynamic load, a percentage estimation error is defined. For the dynamic load, the percentage error at the i^{th} iteration is defined as

$$\frac{||\mathbf{f} - \hat{\mathbf{f}}_i||}{||\mathbf{f}||} \times 100. \tag{29}$$

For each parameter θ_k, the percentage error at the i^{th} iteration is defined as

$$\frac{|\theta_k - \hat{\theta}_{k,i}|}{|\theta_k|} \times 100 \tag{30}$$

The identified dynamic load and bending stiffnesses are shown in Figures 4 and 5. The dynamic load is plotted for different iterations to show its evolution throughout the identification process. The estimation errors for the structural parameters and dynamic load are shown in Figure 6. The percentage error in the identified dynamic load at the last iteration is found to be 0.0243% which is very small and may be neglected. It can be deduced that the algorithm has successfully identified the dynamic load.

Table 2 provides the final values of the identified structural parameters and their final percentage errors. It is also noted that the final error in the identified structural parameters is also very small, which indicate a good convergence and applicability of the proposed method to simultaneously identify structural parameters and dynamic loads.

To validate the accuracy of the identification procedure, the identified structural parameters and dynamic load are used to recompute the dynamic response of the structure for an unmeasured dof, and compare it to the response calculated using the reference model. The linear acceleration response

Table 2: Identified structural parameters and their absolute error.

Parameter	Identified value (Nm^2)	Error(%)
EI_1	2.7937×10^6	0.025
EI_2	1.7531×10^6	0.02
EI_2	5.2557×10^6	0.011

located at 2 m from the left-hand side of the beam is computed using the identified structural parameters and dynamic load. Figure 7 shows the reconstructed acceleration together with reference response computed from the reference values of the structural parameters and dynamic load. It can be seen that the reconstructed response is in a good agreement with the reference response, indicating that the identified dynamic load and structural parameters can be used to predict the dynamic response of the structure at locations where no sensors are installed, and they are representative of the true values of the structural parameters and dynamic load.

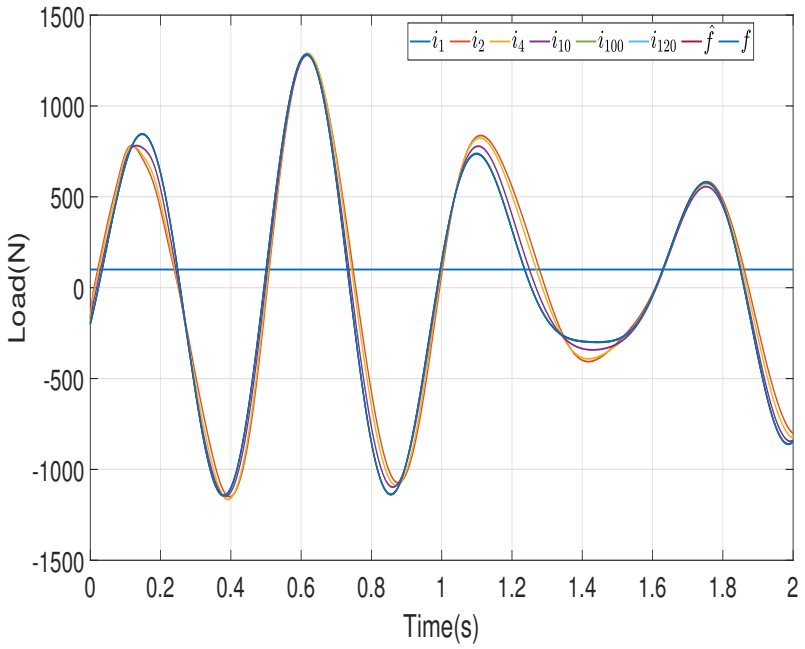

Figure 4: Estimated dynamic load time history at different iterations

3.1.1. Effects of measurement noise

This section will analyse the adverse effects of the measurement noise on the identified structural parameters and dynamic load. For this purpose, a white noise is added to the measured accelerations and displacements. The ratio between the standard deviation of the marginal distribution of this white noise and the mean square of the response over the time interval is denoted by l (in percent). The effects of $l = 1\%$ and $l = 5\%$ noise in the measurements are considered and shown in Figures 8, 9, 10 and 11.

It can be observed that the percentage error increases as the noise level increases in the measured responses. In the case of $l = 1\%$ noise, the identified dynamic load can be seen in Figure 8, and the maximum percentage error over the time interval of analysis is 1.85%, this maximum error increases to 3.86% when the noise level is increased to $l = 5\%$ and Figure 10 shows the dynamic load time history for this case. Figures 9 and 11 show the percentage errors for the structural parameters and dynamic load

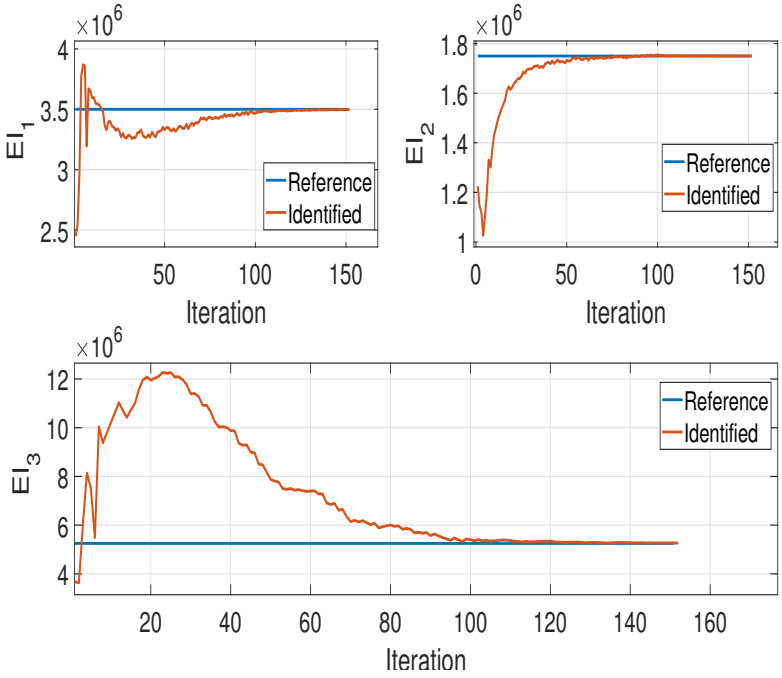

Figure 5: Identified bending stiffnesses

for both cases. The proposed method is capable of a robust simultaneous identification of the structural parameters and dynamic loads even in presence of random noise in the measured responses.

3.1.2. Effects of initial estimates

The effects of initial estimates on the structural parameters and dynamic load are analysed herein. First, the structural parameters are assigned different initial estimates in order to verify the applicability and robustness of the proposed method, the bending stiffnesses are assigned initial estimates of $2.5, 2, 1.5, 0.7, 0.5$ times their true values, and the dynamic load was assigned an initial estimate of 100 N. Figure 12 shows the identified bending stiffness EI_1 for each simulation case. It is clear that in each case, a stable convergence towards the reference value is obtained regardless of the starting initial values. This demonstrates the robustness of the proposed method against initial estimates and its capability to converge to the true values even when the starting estimates are far from the true values. The effects of the initial estimates on the dynamic load are also studied. The dynamic load was assigned initial estimates of $10, 50, 100, 500, 1000$ N which are significantly different from the optimal dynamic load given in Eq.(28), and the structural parameters are given an initial estimate of 60% of their true values in all simulation cases to investigate the effects of initial estimates on the identified dynamic load. Figure 13 shows the estimation of the percentage error in the identified dynamic load in each simulation case. It can be observed that in each case, the dynamic load converges to the optimal solution regardless of the values of the initial estimates.

In addition to the previous analysis, a total of 50 simulation cases were conducted where random initial estimates were assigned to the structural parameter and the dynamic load. For each simulation case, the parameters and the load were assigned a random value between 0.5 and 5 times their true values.The final value of the percentage error of the structural parameters and dynamic load is estimated in each simulation case. Figure 14 shows the final percentage error values estimated for each simulation case. It can be observed that in all cases, the percentage error was bounded and less than 1%, indicating the robustness of the proposed approach to initial estimate.

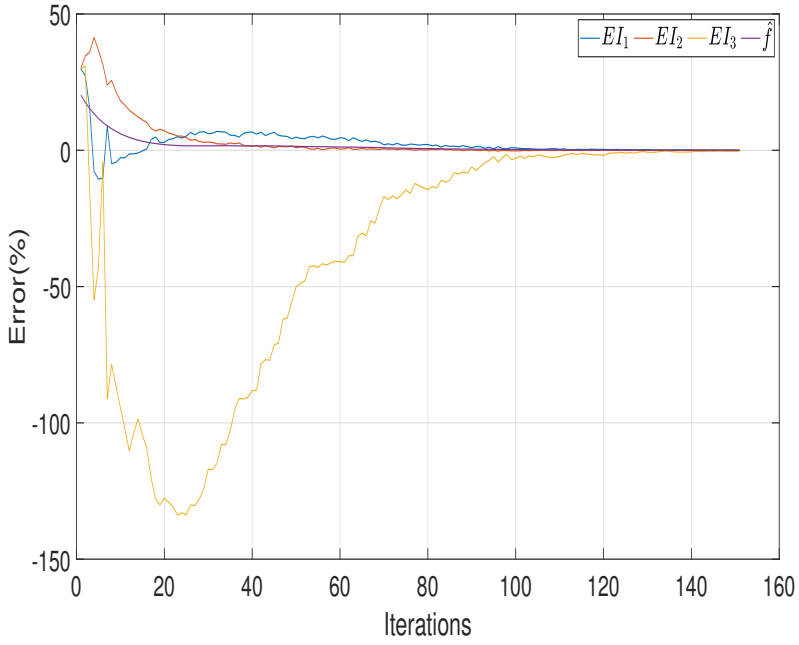

Figure 6: Percentage error estimation

3.2. Truss structure

This section will consider the structure depicted in Figure 15, made up with 21 truss elements and 12 nodes. The total number of dofs is 24. For all the elements, the Young's modulus is $E = 200$ GPa and the cross-sectional area is $A = 10^{-4}\,\mathrm{m}^2$, the mass density is $\rho = 8000\,\frac{\mathrm{Kg}}{\mathrm{m}^3}$. The total horizontal length of the structure is 60 m, and each horizontal member have length of 10 m, and the vertical height is 10 m. A Rayleigh damping model was adopted in this example, such that the damping ratio of the first two elastic modes is $\zeta = 7\%$. The first four natural frequencies of the structure are $7.59\,, 16.42\,, 27.35\,, 30.47\,\mathrm{Hz}$.

In this example, the dynamic load is applied on node 2 (see figure 15) in the downward direction, the dynamic load is a sinusoidal load lasting 0.3 seconds and is expressed as

$$\mathbf{f}(t) = \begin{Bmatrix} 500\sin(10t) & t \leq 0.3 \\ 0 & t > 0.3 \end{Bmatrix}. \tag{31}$$

The dynamic load time history is shown in Figure 16. The response is computed using the Newmark-β method, the reference values of the structural parameters and dynamic load are used to compute the reference (measured) responses, and the response is calculated for one second. The parameters that will be identified in this study are the Young's modulus E, and the damping ratio ζ as well as the time history of the dynamic load. Before starting the identification process, an initial values of structural parameters and dynamic load must be provided, table 3 lists the reference values of the structural parameters and dynamic load as well as their initial estimates which are used in the identification process. The data used for the identification are the vertical displacements of nodes 3 and 6 and the vertical accelerations of nodes 2 ,3 and 4. The convergence of the identified structural parameters and the time history of the dynamic load is shown in figures 17 and 18. The identified dynamic load for several iterations is shown in Figure 17 to demonstrate the estimation of the dynamic load during the identification process. The structural parameters are identified with high accuracy and stable convergence, and the final values of the identified structural parameters and their percentage error estimation are reported in Table 4. The estimation of the percentage errors in the identified structural parameters and dynamic load can also be

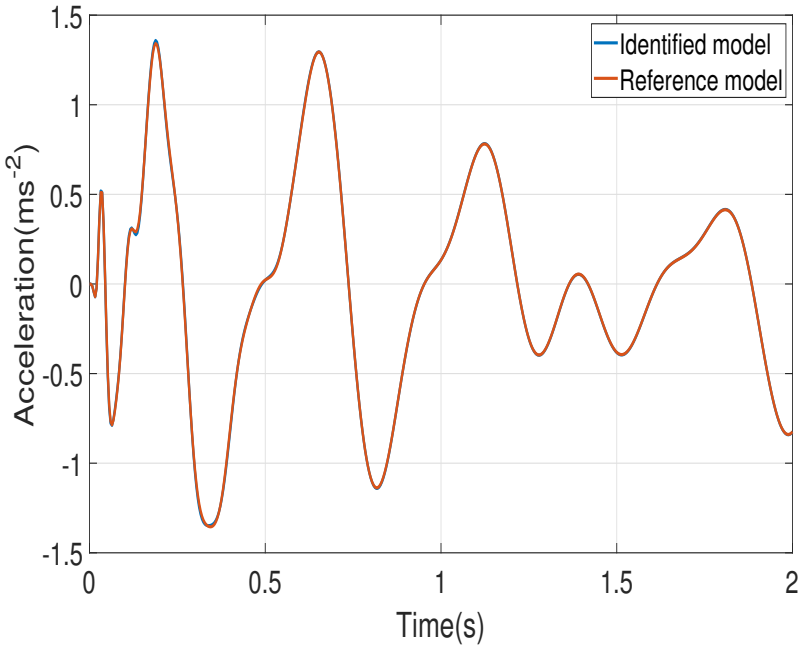

Figure 7: Reconstructed acceleration response.

Table 3: Optimal values and initial estimate of structural parameters and dynamic load

Parameter	Optimal value	Initial estimate
E	200×10^9	100×10^9
ζ	0.07	0.035
$\mathbf{f}(t)$	-	100

seen in Figure 19, clearly all structural parameters and dynamic load converged to the optimal solution, and the maximum percentage error in the identified dynamic load is 0.075% which is very small. It can be concluded that the identified dynamic load and structural parameters are indeed representative of the true values of the dynamic load and structural parameters.

3.2.1. The effects of multiple excitations

In many practical situations, a structure will be excited by more than a single dynamic load, and the simultaneous identification of structural parameters and these dynamic loads is therefore an important task. The same truss structure is considered but it is now excited by two dynamic loads as shown in Figure 20. Both dynamic loads are acting in the downward direction at node 2 and node 6, the load at node 2 is a multi harmonic dynamic load, which can be expressed mathematically as follows

$$\mathbf{f}_1(t) = -2000\sin(20t) + 3000\sin(25t) - 4000\cos(33t) + 500\cos(35t). \tag{32}$$

Table 4: Identified structural parameters and their percentage error

Parameter	Identified value	Error(%)
E	1.9990×10^9	0.086
ζ	0.06999	0.179

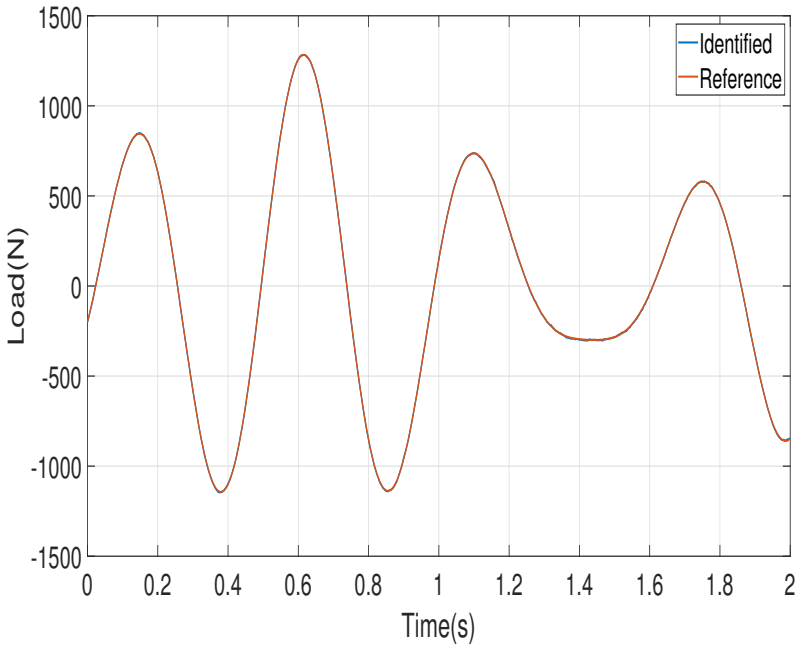

Figure 8: Identified dynamic load time history for noisy case of $l = 1\%$.

The second dynamic load is the same as the dynamic load given in Eq.(31). The damping ratio is assumed to be known and will not be identified, and the Young's modulus is chosen to be identified simultaneously with the two dynamic load time histories, the initial estimate of the structural parameter is set to 60% of their true value, and both dynamic loads are given an arbitrary initial constant value of 1000 N, which is completely different from the optimal dynamic loads given by Eq. (32) and (31). Figures 21 and 22 shows the time history of the estimated dynamic loads for several iterations. It can be observed from the previous figures that the method is capable of identifying simultaneously the structural parameters and dynamic loads even when the structure is excited by multiple dynamic loads. The percentage error in the identified Young's modulus is very small and it is found to be 0.12% which is almost equal to the true value provided in table 3; the identified dynamic loads are also very close to the true dynamic loads and the percentage error estimation of the dynamic loads can be seen in Figure 24. It is clear that at the beginning of the identification process, the identified dynamic loads greatly differ from the true dynamic loads, and as the number of iterations increases, the identified dynamic loads gradually converge towards the true dynamic loads. The final values of the percentage error in both dynamic loads are respectively 0.09% and 0.16%. To conclude, the proposed method is shown to produce a satisfactory simultaneous identification results, and it was also tested for more general cases where the structural system is excited by multiple dynamic loads, and it was capable to achieve a good results as demonstrated by the previous analysis.

3.2.2. Effects of the number of measurements

The effects of the number of measurements on the rate of convergence are analysed in this section. The same structure (depicted in Figure 20) with two dynamic loads is considered. Five different cases for the numbers and locations of the measurements are considered and listed in Table 5. In this table the measured dofs are listed sequentially. Therefore odd numbers indicates the horizontal direction and even numbers indicates the vertical direction. The convergence of the identified Young's modulus in each case is shown in Figure 25. It is clear that for the first 3 cases, the identified Young's modulus is not close to the true value; however, as the number of measurements increases, the identified value converges to the true value, and it can also be observed that in the last two cases, the same solution

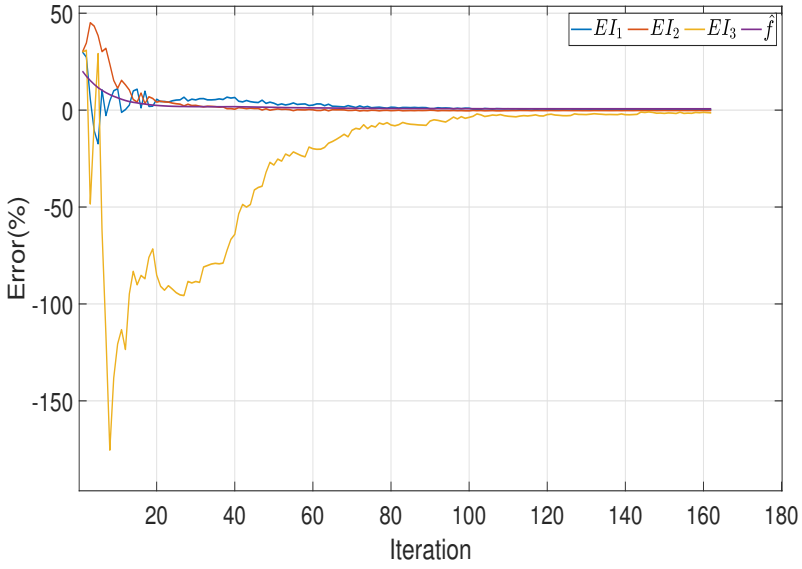

Figure 9: Percentage Error evaluation $l = 1\%$.

Table 5: Measurement points in each simulation case

Case No.	Acceleration dof	Displacement dof
1	$6, 14$	1
2	$4, 6, 14$	$1, 6$
3	$2, 4, 8, 6, 14$	$1, 8$
4	$2, 4, 8, 6, 14, 15, 17$	$1, 8$
5	$2, 4, 8, 6, 10, 12, 14, 16,$	$1, 9, 19$

is obtained even if more sensors(measurements) are used in the identification process. Therefore, it is important to select an appropriate number of measurements to guarantee an optimal solution and reduce the computational cost associated with installing more sensors. In this example, it is found that using 8 measurements will lead to the optimal solution without reducing the computational accuracy of the identification process. Furthermore, adding more measurements does not significantly improve the solution. In general, using more sensors (measurements) in the identification procedure will yield more satisfactory results. Nevertheless, it not always possible to install more sensors on the structural system due to practical and financial limitations. The impact of the location (and not the number) of measurements will be considered in further research in order to provide a guidance on where to place them.

4. Experimental validation

In this section the proposed approach is validated using 3-storey structure equipped with accelerometers. The structure is depicted in Figure 26. The real structure is made up from 4 aluminium blocks, all blocks have length of 0.2 m, width of 0.15 m and the the thickness of all blocks is 0.02 m. The lowest block is clamped to the ground. The remaining blocks are equipped with accelerometers, the top block is excited with a hammer along x-direction. The test rig and the experimental data used in this section were presented in [2] in a previous research. The true impact dynamic load time history is shown in Figure 27. The structure was modelled numerically using 3-dof mass-spring-damper system depicted in Fig. 28, the axial and torsional deformation of the structure was assumed negligible during

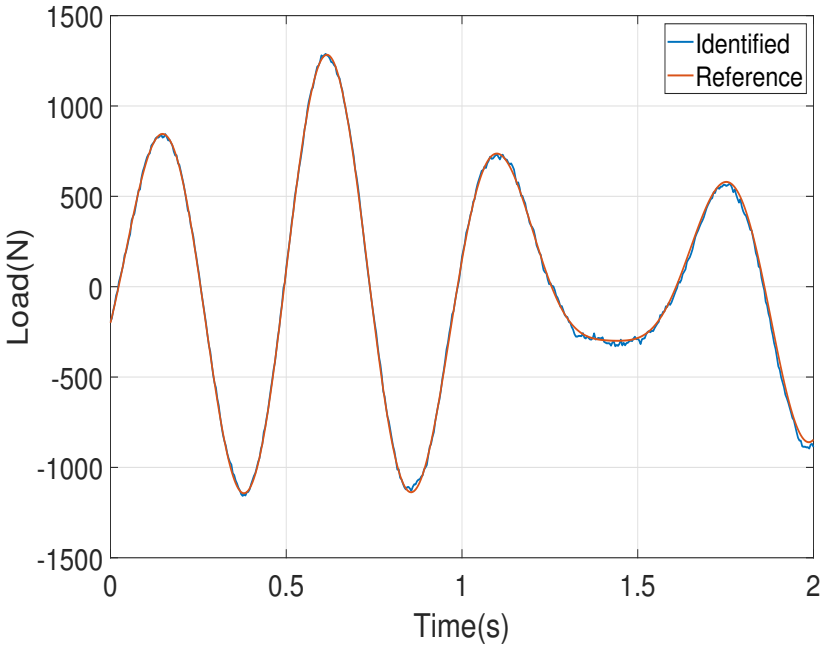

Figure 10: Identified dynamic load time history for noisy case of $l = 5\%$

the modelling process. The masses of the plates are $m_1 = 1.47$ kg, $m_2 = 1.52$ kg and $m_3 = 1.54$ kg. The masses are assumed known and will not be identified in this experimental investigation. A viscous damping model was adopted, the damping and stiffness parameters are respectively c_1=1.1946 Ns/m, c_2=1.14338 Ns/m, c_3=0.6189 Ns/m, $k_1 = k_3 1.41 \times 10^4$ N/m and k_2=1.3 $\times 10^4$ N/m. In [2], in which another model updating was presented, the stiffnesses and modal damping ratios were used as updating parameters. The acceleration response and the dynamic load time history were recorded simultaneously using accelerometers and force gauge in the hammer, the displacement and the velocity were then computed via numerical integration. To mitigate the effect of measurement noise in the measured acceleration signals, a high pass filter was used with cut-off frequency of 2 Hz. The sampling frequency is 256 Hz, and the excitation was applied on the third floor along x-direction. The measured acceleration and the integrated displacements are depicted in the figures 29 and 30.

4.1. Identification results

The proposed approach was used to identify simultaneously the structural parameters and dynamic load, the acceleration of the 3^{rd} mass and the integrated displacement of the 1^{st} mass were used in the identification. A different validation strategy will be used compared to the previous numerical examples. Since there are no reference values for the structural parameters, the most appropriate way to validate the identified structural parameters and dynamic load is to use them to reconstruct the acceleration response and compare it with the measured acceleration response. Nevertheless, for the stiffnesses, table 6 provides a comparison between the identified structural parameters and the updated parameters from [2]. The stiffness parameters agrees quite well with the updated parameters found in [2]. Figures 31 and 32, show the convergence of the identified stiffnesses and damping parameters of the second and third masses. The identified dynamic load is depicted in the Figure 33. It can be observed that the identified dynamic load is very close to the measured dynamic load as indicated by the peak value. It should also be noted that the initial estimate given to the dynamic load was 1 N for all time history to start the identification process, which is significantly different from the real measured excitation. The maximum percentage error in the identified dynamic load was found to be 8.33% which is completely

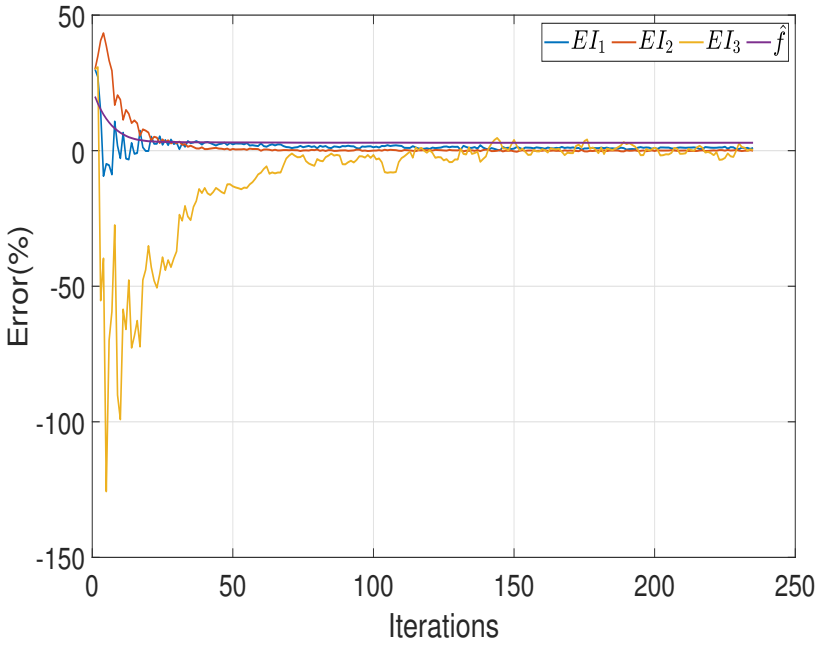

Figure 11: Percentage Error evaluation $l = 5\%$.

Table 6: Comparison between the identified parameters and the reference values in [2].

Parameter	Value in [2]	Identified value	error(%)
k_1 (N/m)	14100	13933	1.1844
k_2 (N/m)	13100	13101	0.8
k_3 (N/m)	14100	14021	0.8

acceptable for engineering application. Furthermore, to illustrate the effect of the low frequency drift on the identified dynamic load and the necessity to use data fusion method, the identification procedure has been done using only acceleration measurements. Figure 34 shows the corresponding identified loadIt can be clearly observed that the identified load using acceleration measurements only will lead to a drift in the identified dynamic load. The data fusion method of acceleration and displacement is therefore more robust to this drift caused by the high frequency component in the acceleration measurements.
To validate the identification precedure, the acceleration signals were reconstructed using the identified parameters and loads, and compared with the measured acceleration signals provided in 29. It can be observed that the reconstructed signals using the identified parameters and loads agree well with the measured acceleration signals with small discrepancy between the two models which is expected and acceptable. Therefore, it can be concluded that the identified parameters and dynamic load can indeed be used to represent the real structure as indicated by the reconstructed acceleration signals. Hence, the proposed approach can simultaneously identify the dynamic loads and structural parameters. It should noted that the numerical model used here (discrete model) is not a perfect representation of the real system, yielding modelling error. An accurate FE model would certainly improve the results. Furthermore, displacement transducers may also be used along with accelerometers to directly obtain the displacement measurements, this will avoid the accumulation of errors due to the numerical integration of the acceleration and velocity signals.

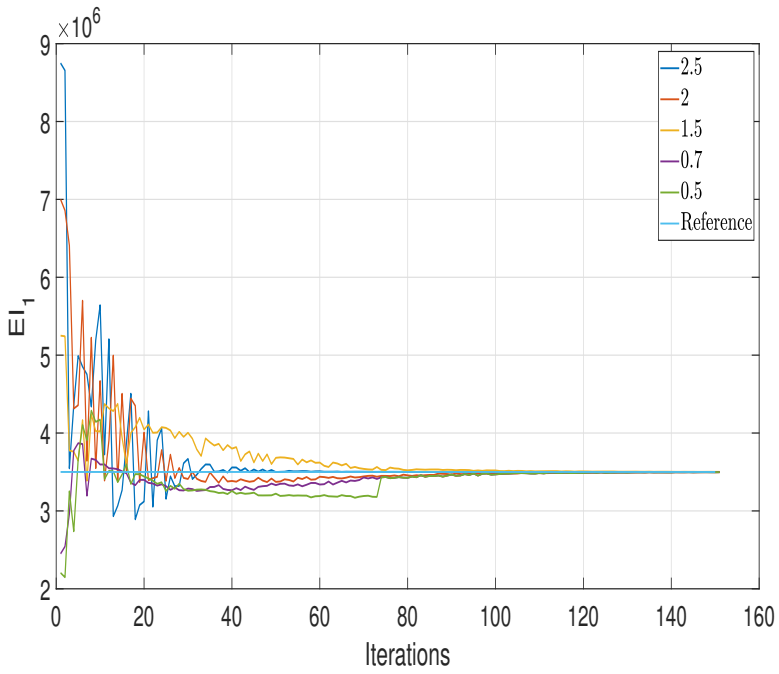

Figure 12: Identified EI_1

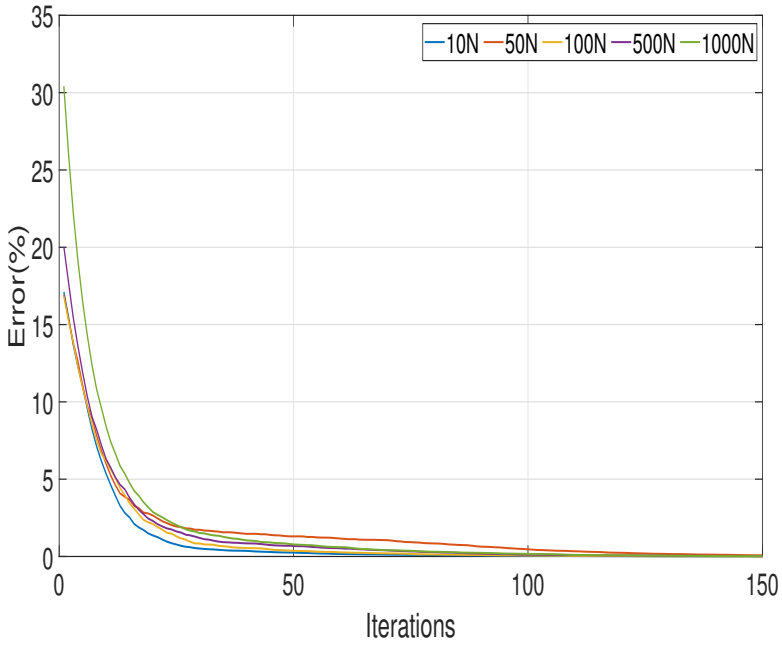

Figure 13: Error evaluation of the identified dynamic load

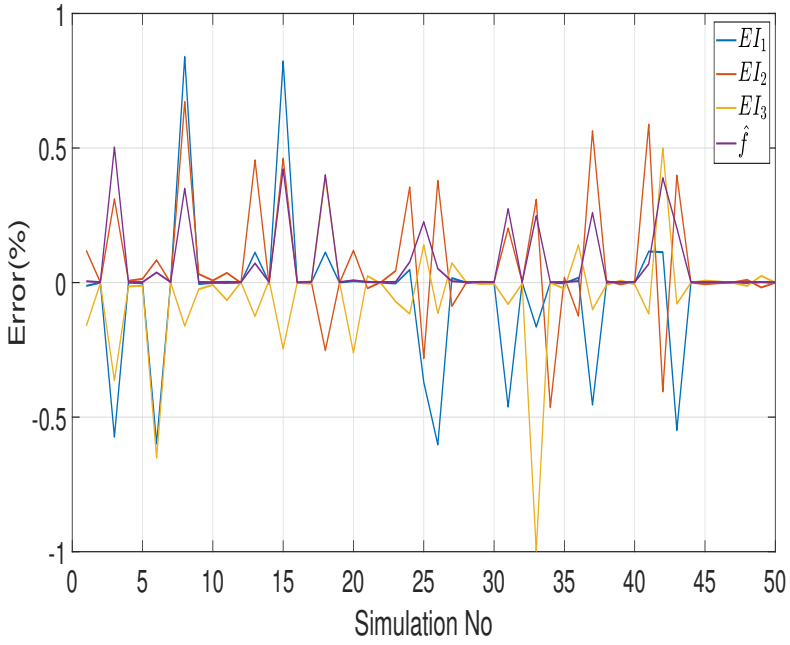

Figure 14: Percentage error for 50 simulation cases

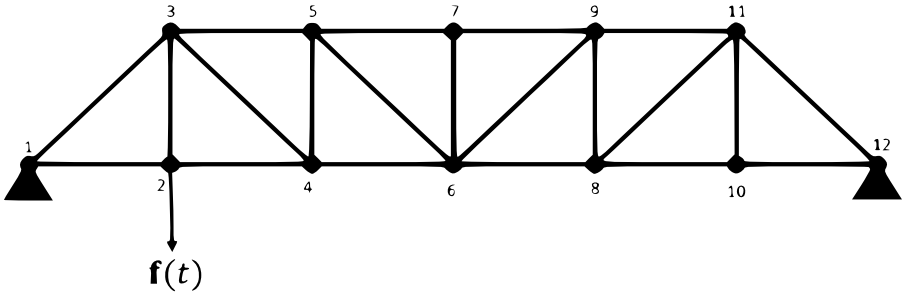

Figure 15: FE model of truss structure

5. Conclusions

In summary, a novel algorithm is proposed in this paper to simultaneously identify structural parameters and dynamic loads from a limited set of measured structural responses. The method is based on the use of the Levenberg-Marquardt method to update, at each iteration, sequentially the structural parameters and dynamic loads. Data fusion of acceleration and displacement responses is used to reduce the effect of low-frequency drift on the identified dynamic load. Several numerical examples are used to demonstrate the effectiveness and robustness of the proposed method. In particular, the effect of the measurement noise, the initial values and the number of measurements on the accuracy and convergence of the proposed method is analysed. Good results are obtained even when the structure is excited by multiple dynamic loads. Finally, the proposed approach was validated experimentally using 3-storey structure, in which the dynamic load and the structural parameters were identified simultaneously.

Concerning the shortcomings of the proposed approach, the proposed approach as presented in this paper can only be used for linear structures. The extension to non-linear structures requires a different formulation that will be investigated in future works. The proposed approach is optimal when using both measurements of acceleration and displacement which may not always be experimentally feasible, and

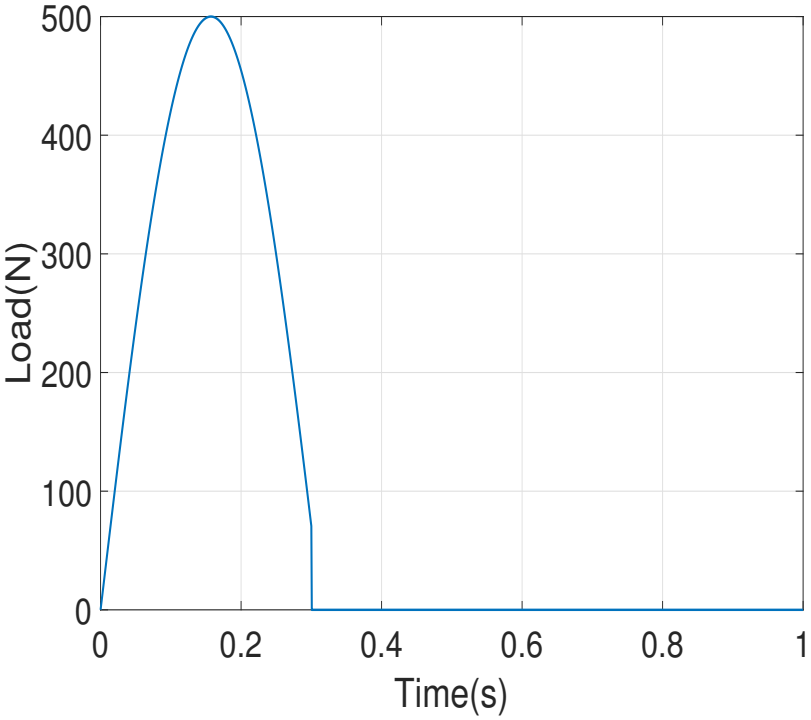

Figure 16: Dynamic load time history

the integration of the acceleration signals to obtain the displacement measurements is not recommended.

5.1. Acknowledgement

The first author Z.Bitro kindly acknowledges financial support by the Libyan embassy to enable this work to be published.

References

[1] Onur Avci, Osama Abdeljaber, Serkan Kiranyaz, Mohammed Hussein, Moncef Gabbouj, and Daniel J. Inman. A review of vibration-based damage detection in civil structures: From traditional methods to machine learning and deep learning applications. *Mechanical Systems and Signal Processing*, 147:107077, 2021.

[2] Anas Batou. A sensitivity-based one-parameter-at-a-time model updating method. *Mechanical Systems and Signal Processing*, 122:247–255, 2019.

[3] Pankaj Chaupal and Prakash Rajendran. A review on recent developments in vibration-based damage identification methods for laminated composite structures: 2010–2022. *Composite Structures*, 311:116809, 2023.

[4] Jun Chen and Jancie Li. Simultaneous identification of structural parameters and input time history from output-only measurements. *Computational Mechanics*, 33(5):365–374, 2004.

[5] Zhidan Chen, Shun Weng, Hong Yu, Jiajing Li, Hongping Zhu, Yongyi Yan, and Liying Wu. Bayesian-based method for the simultaneous identification of structural damage and moving force. *Mechanical Systems and Signal Processing*, 185:109742, 2023.

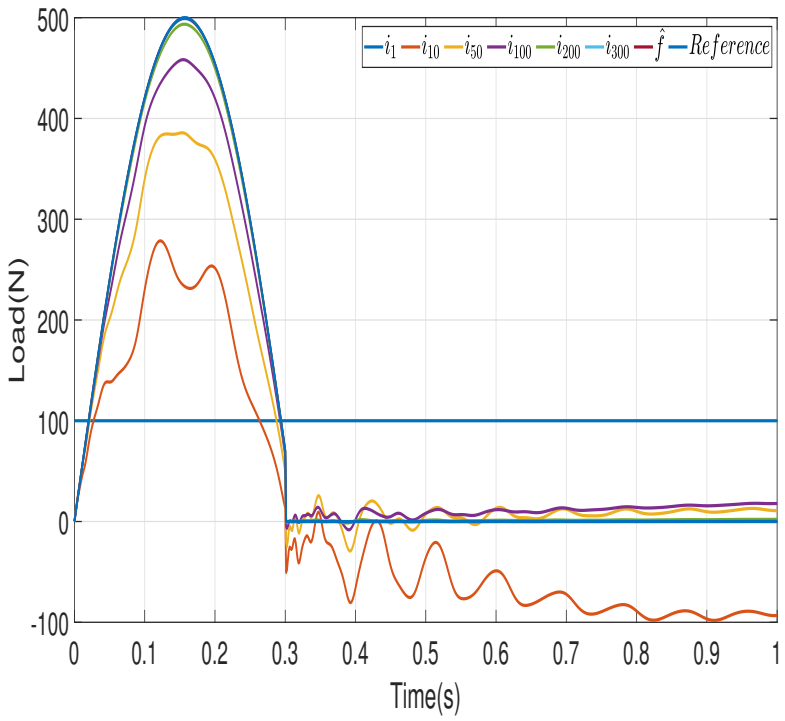

Figure 17: Estimated dynamic load time history at different iterations

[6] Alberto Corigliano and Stefano Mariani. Parameter identification in explicit structural dynamics: performance of the extended kalman filter. *Computer Methods in Applied Mechanics and Engineering*, 193(36):3807–3835, 2004.

[7] Miao Cui, Yi Zhao, Bingbing Xu, and Xiao wei Gao. A new approach for determining damping factors in levenberg-marquardt algorithm for solving an inverse heat conduction problem. *International Journal of Heat and Mass Transfer*, 107:747–754, 2017.

[8] Yong Ding, B Y Zhao, and B Wu. Structural system identification with extended kalman filter and orthogonal decomposition of excitation. *Mathematical Problems in Engineering*, 2014:987694, 2014.

[9] Scott W Doebling, Charles R Farrar, Michael B Prime, et al. A summary review of vibration-based damage identification methods. *Shock and vibration digest*, 30(2):91–105, 1998.

[10] Jinyan Fan and Jianyu Pan. A note on the levenberg–marquardt parameter. *Applied Mathematics and Computation*, 207(2):351–359, 2009.

[11] Dongming Feng and Maria Q. Feng. Identification of structural stiffness and excitation forces in time domain using noncontact vision-based displacement measurement. *Journal of Sound and Vibration*, 406:15–28, 2017.

[12] Dongming Feng, Hao Sun, and Maria Q. Feng. Simultaneous identification of bridge structural parameters and vehicle loads. *Computers & Structures*, 157:76–88, 2015.

[13] Qin Huang, Yei L. Xu, and Hou J. Liu. An efficient algorithm for simultaneous identification of time-varying structural parameters and unknown excitations of a building structure. *Engineering Structures*, 98:29–37, 2015.

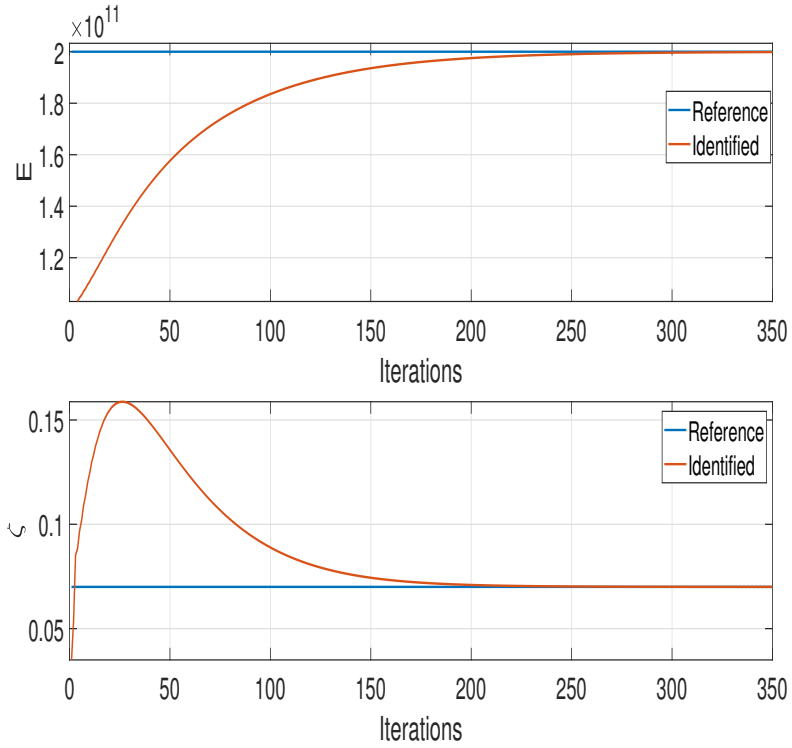

Figure 18: Identified structural parameters

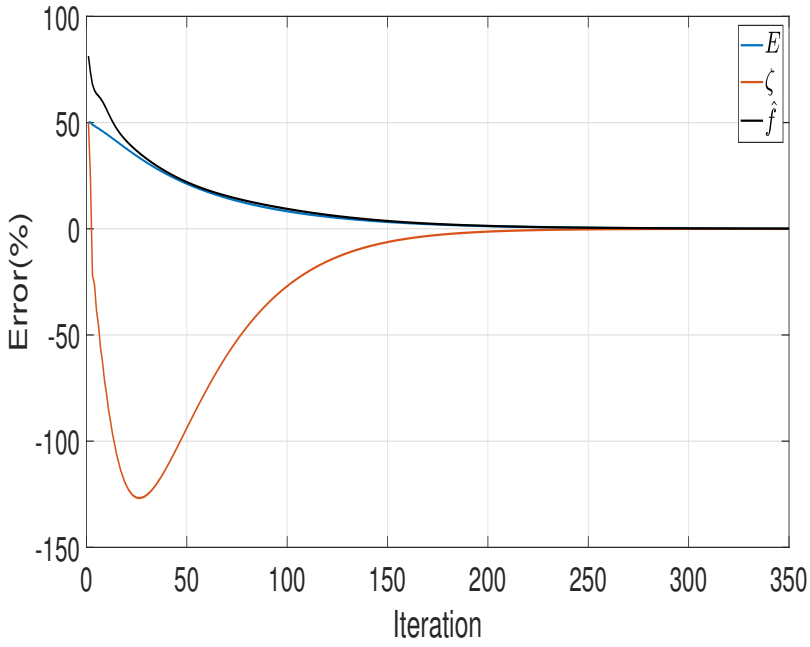

Figure 19: Error evaluation of structural parameters and dynamic load

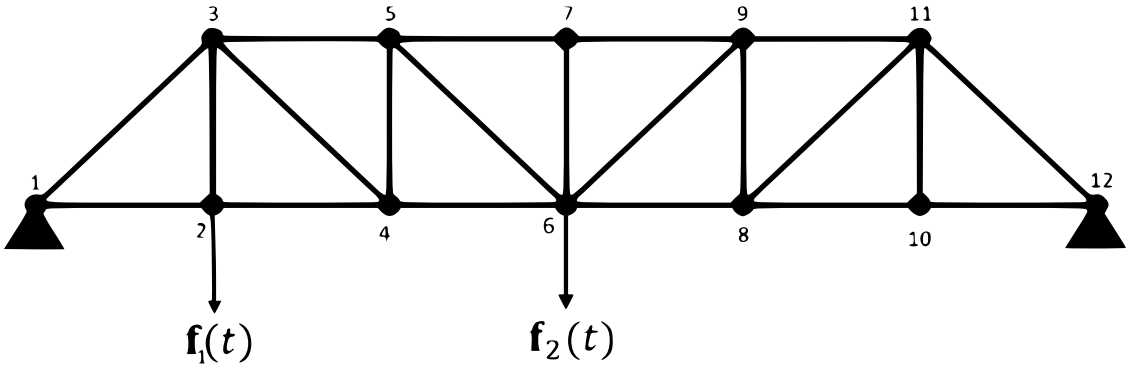

Figure 20: FE model of a truss structure with two excitations

[14] Jayalakshmi and Rama Mohan Rao. Simultaneous identification of damage and input dynamic force on the structure for structural health monitoring. *Structural and Multidisciplinary Optimization*, 55(6):2211–2238, 2017.

[15] Jing Ji, Maomao Yang, Liangqin Jiang, Jia He, Zhenchao Teng, Yingchun Liu, and Huayu Song. Output-only parameters identification of earthquake-excited building structures with least squares and input modification process. *Applied Sciences*, 9(4), 2019.

[16] Hasan Katkhuda and Achintya Haldar. A novel health assessment technique with minimum information. *Structural Control and Health Monitoring*, 15(6):821–838, 2008.

[17] Hasan Katkhuda, Rene Martinez, and Achintya Haldar. Health assessment at local level with unknown input excitation. *Journal of Structural Engineering*, 131(6):956–965, 2005.

[18] Yunwoo Lee, Heesoo Kim, Seongi Min, and Hyungchul Yoon. Structural damage detection using deep learning and fe model updating techniques. *Scientific Reports*, 13(1):18694, Oct 2023.

[19] Lijun Liu, Wei Hua, and Ying Lei. Real-time simultaneous identification of structural systems and unknown inputs without collocated acceleration measurements based on mekf-ui. *Measurement*, 122:545–553, 2018.

[20] Lijun Liu, Ying Su, Jiajia Zhu, and Ying Lei. Data fusion based ekf-ui for real-time simultaneous identification of structural systems and unknown external inputs. *Measurement*, 88:456–467, 2016.

[21] Zhongrong Lu and Cess Law. Identification of system parameters and input force from output only. *Mechanical Systems and Signal Processing*, 21(5):2099–2111, 2007.

[22] Changfeng Ma and Lihua Jiang. Some research on levenberg–marquardt method for the nonlinear equations. *Applied Mathematics and Computation*, 184(2):1032–1040, 2007.

[23] Donald W. Marquardt. An algorithm for least-squares estimation of nonlinear parameters. *Journal of the Society for Industrial and Applied Mathematics*, 11(2):431–441, 1963.

[24] John E. Mottershead, Michael Link, and Michael I. Friswell. The sensitivity method in finite element model updating: A tutorial. *Mechanical Systems and Signal Processing*, 25(7):2275–2296, 2011.

[25] Chudong Pan, Yupeng Qiu, Xun Jiang, and Sixue Peng. Simultaneous identification of impact force and structural local damage under pre-segmentation of structural elements. *Structures*, 57:105186, 2023.

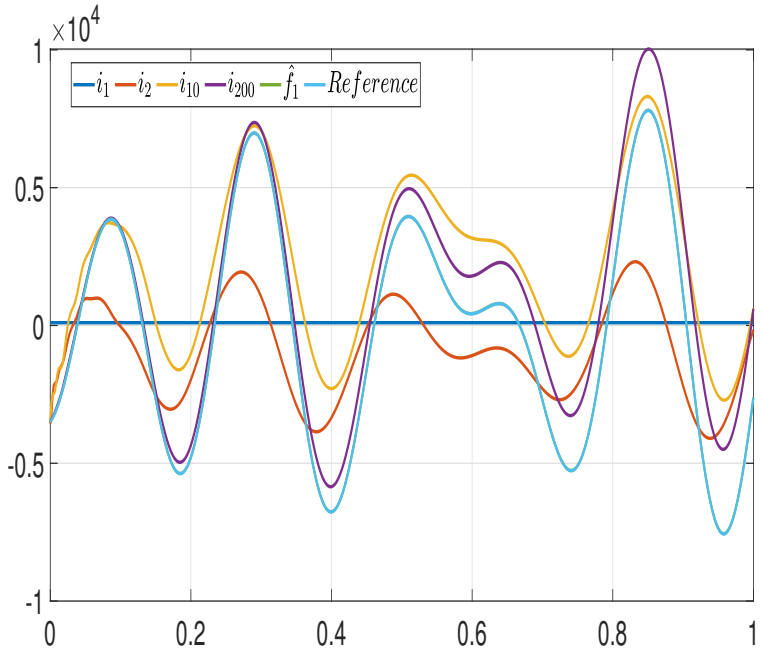

Figure 21: First identified dynamic load time history for several iterations

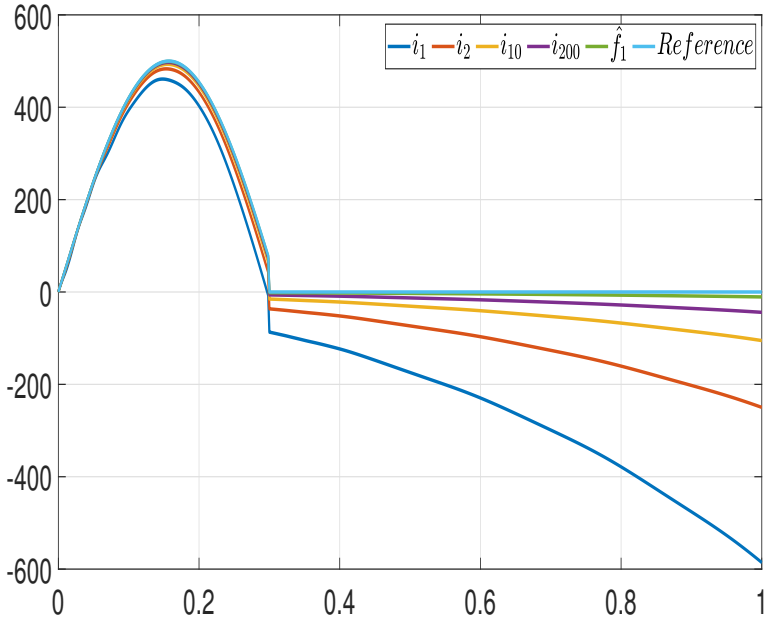

Figure 22: Second identified dynamic load history for several iterations

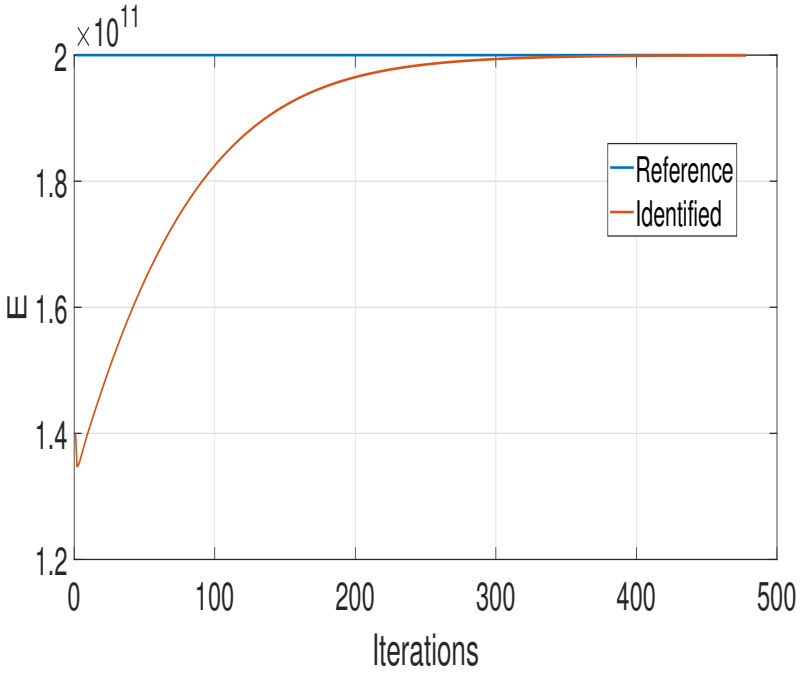

Figure 23: Identified structural parameter

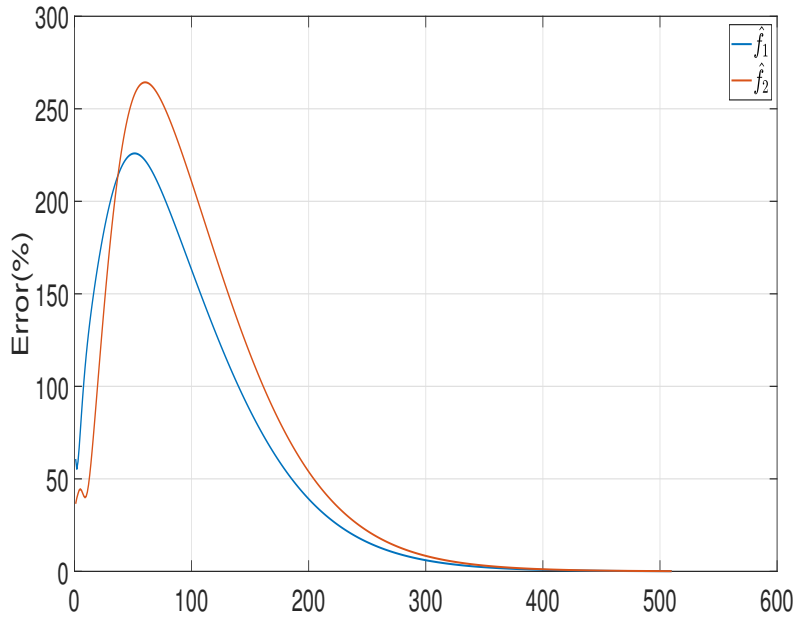

Figure 24: Error evaluation of the dynamic loads

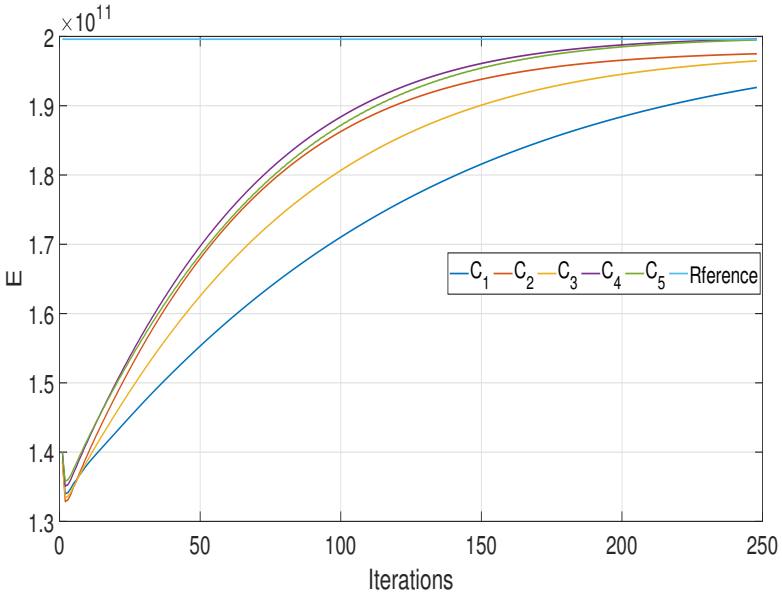

Figure 25: Identified structural parameters in each case

Figure 26: 3-Storey structure

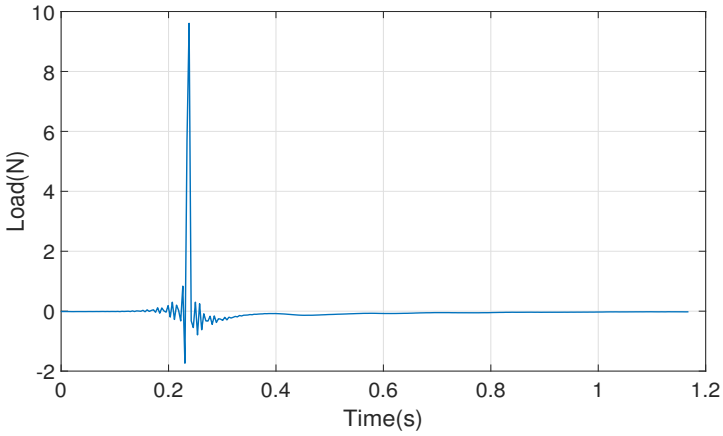

Figure 27: Impact load time history

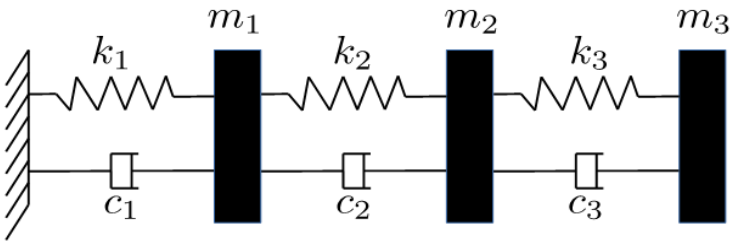

Figure 28: Numerical model

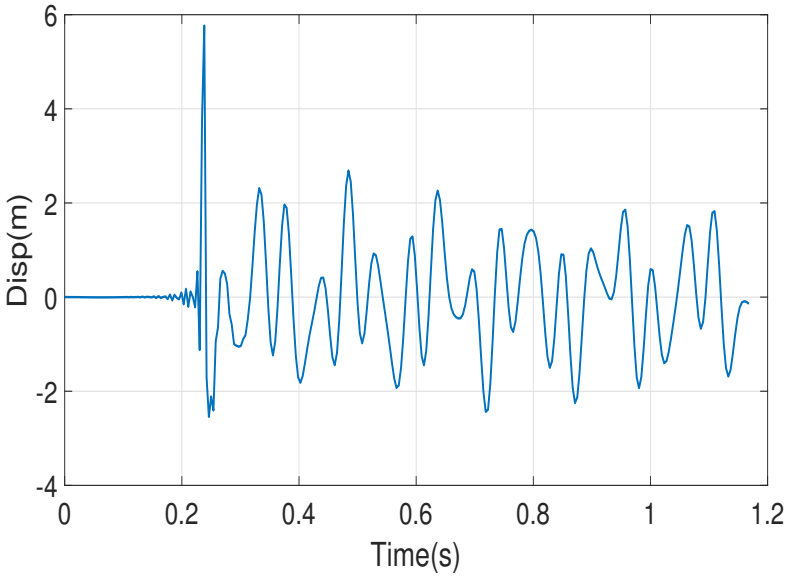

Figure 29: Acceleration measurement on the third mass

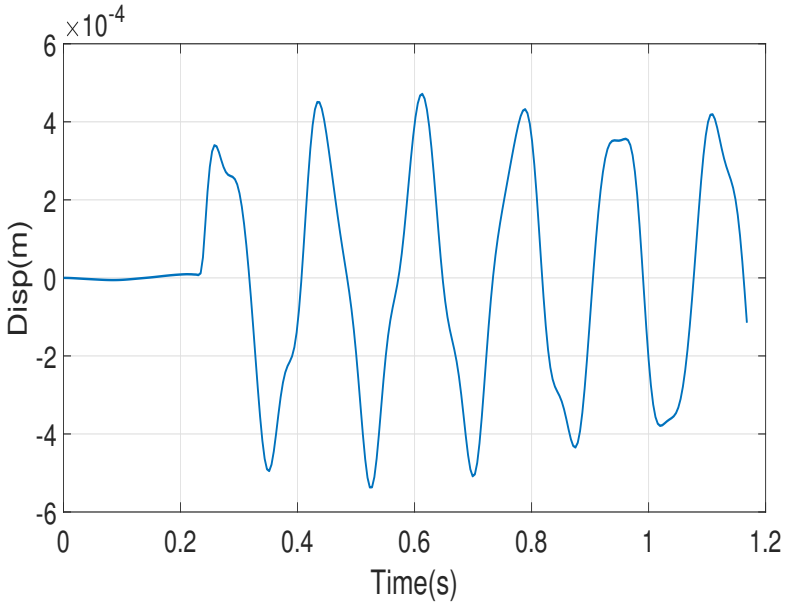

Figure 30: Displacement measurements of the third mass

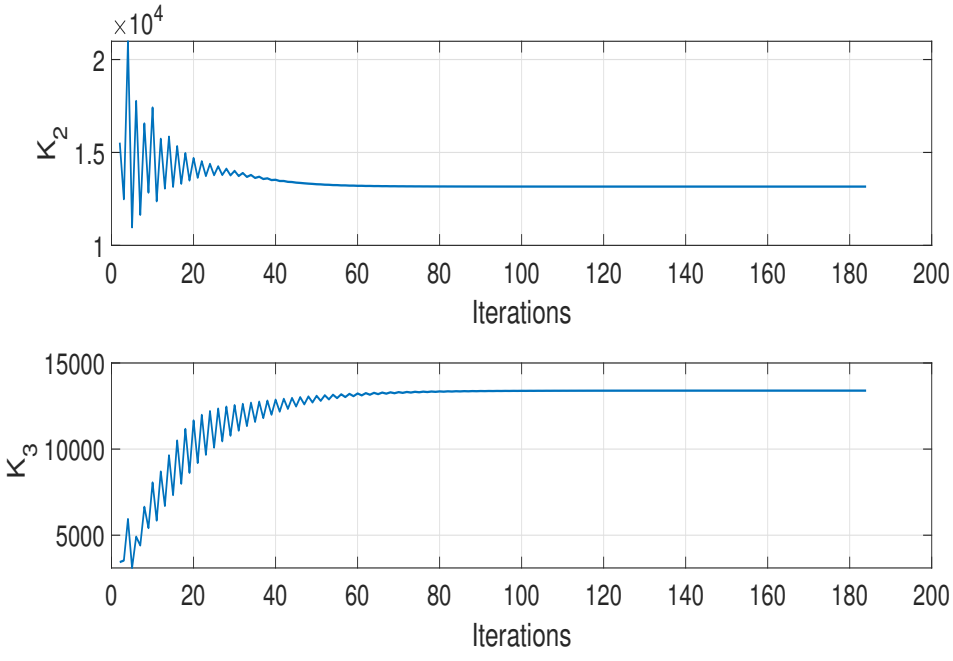

Figure 31: Identified stiffness parameters

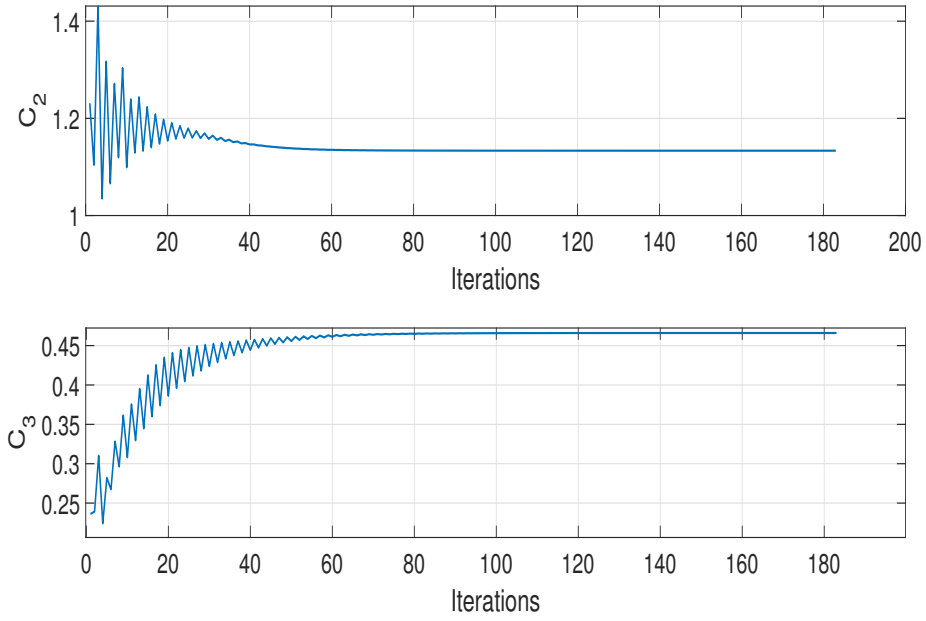

Figure 32: Identified damping parameters

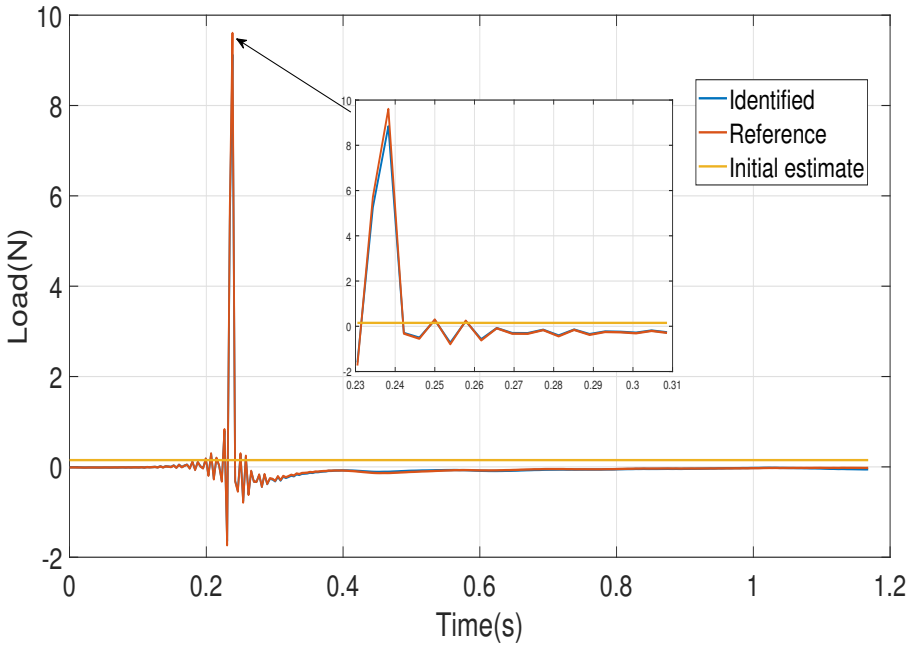

Figure 33: Identified dynamic load

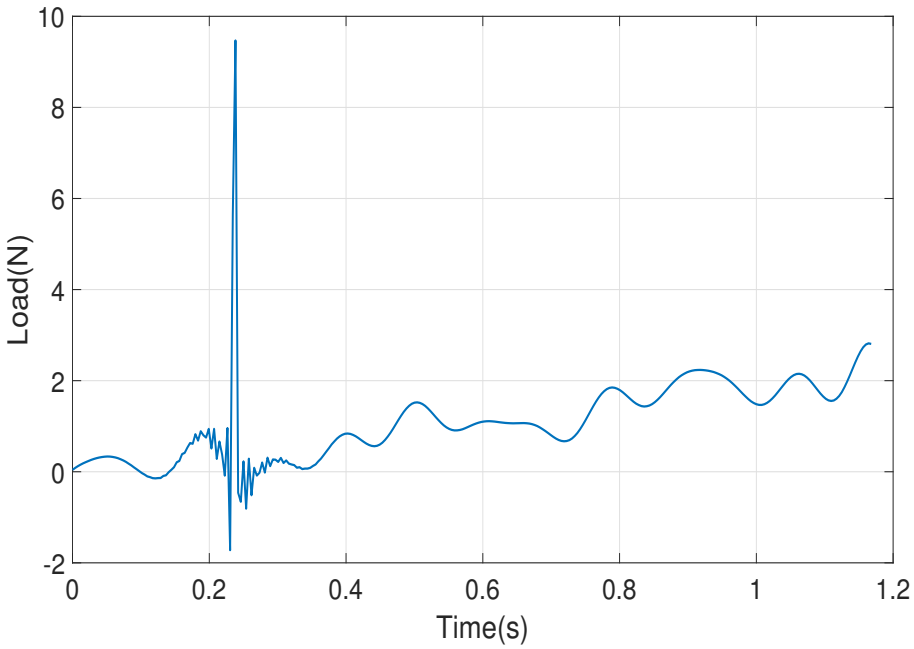

Figure 34: Identified loads using accelerations only

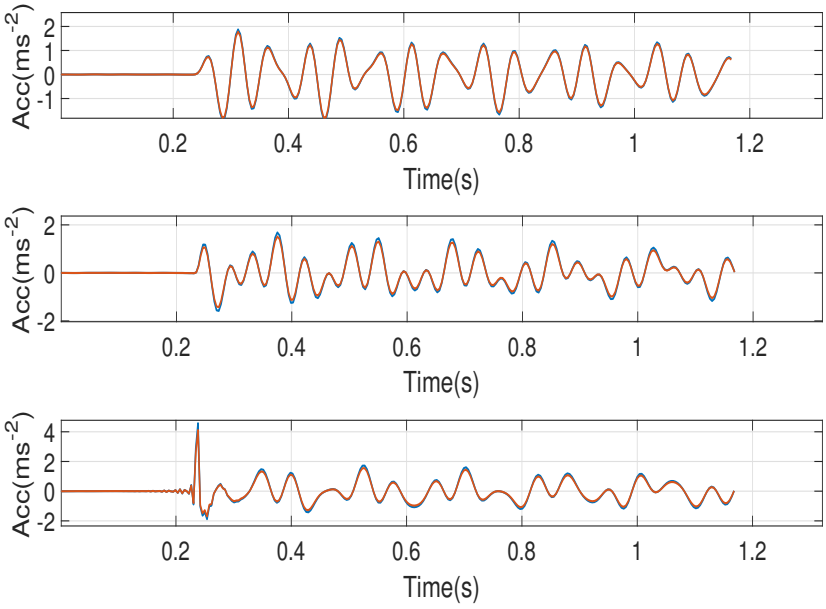

Figure 35: Comparison between the measured and the reconstructed acceleration

[26] Shuwen Pan, Duo Xiao, Shutao Xing, S.S. Law, Pengying Du, and Yanjun Li. A general extended kalman filter for simultaneous estimation of system and unknown inputs. *Engineering Structures*, 109:85–98, 2016.

[27] Solmaz Pourzeynali, Xinqun Zhu, Ali Ghari Zadeh, Maria Rashidi, and Bijan Samali. Simultaneous identification of bridge structural damage and moving loads using the explicit form of newmark-beta; method: Numerical and experimental studies. *Remote Sensing*, 14(1), 2022.

[28] Fariba Shadan, Faramarz Khoshnoudian, and Akbar Esfandiari. A frequency response-based structural damage identification using model updating method. *Structural Control and Health Monitoring*, 23(2):286–302, 2015.

[29] Hao Sun and Raimondo Betti. Simultaneous identification of structural parameters and dynamic input with incomplete output-only measurements. *Structural Control and Health Monitoring*, 21(6):868–889, 2014.

[30] Hao Sun, Dongming Feng, Yang Liu, and Maria Q. Feng. Statistical regularization for identification of structural parameters and external loadings using state space models. *Computer-Aided Civil and Infrastructure Engineering*, 30(11):843–858.

[31] Hongzhi Tang, Jinhui Jiang, M. Shadi Mohamed, Fang Zhang, and Xu Wang. Dynamic load identification for structures with unknown parameters. *Symmetry*, 14(11), 2022.

[32] Chongwen Wang and Chengbin Du. An improved sensitivity method for the simultaneous identification of unknown parameters and external loads of nonlinear structures. *Shock and Vibration*, 2018:1737594, 2018.

[33] Chongwen Wang, Chengbin Du, and Shouyan Jiang. Simultaneous identification of the load and unknown parameters of the structure based on the perturbation method. *Advances in Mechanical Engineering*, 10(10):1687814018805664, 2018.

[34] Duan Wang and Achintya Haldar. System identification with limited observations and without input. *Journal of Engineering Mechanics*, 123(5):504–511, 1997.

[35] Bin Xu, Jia He, Roger Rovekamp, and Shirley J. Dyke. Structural parameters and dynamic loading identification from incomplete measurements: Approach and validation. *Mechanical Systems and Signal Processing*, 28:244–257, 2012.

[36] Hongji Yang, Jinhui Jiang, Guoping Chen, and Jiamin Zhao. Dynamic load identification based on deep convolution neural network. *Mechanical Systems and Signal Processing*, 185:109757, 2023.

[37] Kun Zhang, Hui Li, Zhongdong Duan, and Ces S. Law. A probabilistic damage identification approach for structures with uncertainties under unknown input. *Mechanical Systems and Signal Processing*, 25(4):1126–1145, 2011.

[38] Queng Zhang, Łui Jankowski, and Zhu Duan. Simultaneous identification of excitation time histories and parametrized structural damages. *Mechanical Systems and Signal Processing*, 33:56–68, 2012.

[39] Hongpeng Zhou, Chahine Ibrahim, Wei Xing Zheng, and Wei Pan. Sparse bayesian deep learning for dynamic system identification. *Automatica*, 144:110489, 2022.

[40] Hong-Ping Zhu, Ling Mao, and Shun Weng. A sensitivity-based structural damage identification method with unknown input excitation using transmissibility concept. *Journal of Sound and Vibration*, 333(26):7135–7150, 2014.